RESEARCH ARTICLE

Full spectrum flow cytometry reveals mesenchymal heterogeneity in first trimester placentae and phenotypic convergence in culture, providing insight into the origins of placental mesenchymal stromal cells

Anna Leabourn Boss[1,2]*, Tanvi Damani[2], Tayla J Wickman[1], Larry W Chamley[1], Joanna L James[1†], Anna ES Brooks[2,3†]

[1]Department of Obstetrics and Gynaecology, Faculty of Medical and Health Sciences, University of Auckland, Auckland, New Zealand; [2]School of Biological Sciences, University of Auckland, Auckland, New Zealand; [3]Maurice Wilkins Centre, University of Auckland, Auckland, New Zealand

Abstract Single-cell technologies (RNA-sequencing, flow cytometry) are critical tools to reveal how cell heterogeneity impacts developmental pathways. The placenta is a fetal exchange organ, containing a heterogeneous mix of mesenchymal cells (fibroblasts, myofibroblasts, perivascular, and progenitor cells). Placental mesenchymal stromal cells (pMSC) are also routinely isolated, for therapeutic and research purposes. However, our understanding of the diverse phenotypes of placental mesenchymal lineages, and their relationships remain unclear. We designed a 23-colour flow cytometry panel to assess mesenchymal heterogeneity in first-trimester human placentae. Four distinct mesenchymal subsets were identified; $CD73^+CD90^+$ mesenchymal cells, $CD146^+CD271^+$ perivascular cells, $podoplanin^+CD36^+$ stromal cells, and $CD26^+CD90^+$ myofibroblasts. $CD73^+CD90^+$ and podoplanin + CD36+ cells expressed markers consistent with cultured pMSCs, and were explored further. Despite their distinct ex-vivo phenotype, in culture $CD73^+CD90^+$ cells and $podoplanin^+CD36^+$ cells underwent phenotypic convergence, losing CD271 or CD36 expression respectively, and homogenously exhibiting a basic MSC phenotype ($CD73^+CD90^+CD31^-CD144^-CD45^-$). However, some markers (CD26, CD146) were not impacted, or differentially impacted by culture in different populations. Comparisons of cultured phenotypes to pMSCs further suggested cultured pMSCs originate from $podoplanin^+CD36^+$ cells. This highlights the importance of detailed cell phenotyping to optimise therapeutic capacity, and ensure use of relevant cells in functional assays.

Editor's evaluation

Placental mesenchymal stromal cells (pMSCs) are of interest in therapeutic applications. These cells are typically generated by culturing cells isolated from the villous core of the placenta. However, the villous core is comprised of multiple cell types and the heterogeneity of these cells is often not considered. Consequently, the origin of pMSCs under commonly used culture conditions remains unclear. In the present study the authors have used sophisticated flow cytometry analysis to characterize the heterogeneity of subtypes in the placental villus core in the first trimester of gestation and present convincing data that a specific subpopulation identified likely corresponds to pMSCs in

***For correspondence:** a.boss@auckland.ac.nz

[†]These authors contributed equally to this work

Competing interest: The authors declare that no competing interests exist.

Funding: See page 19

Preprinted: 23 December 2021
Received: 23 December 2021
Accepted: 01 August 2022
Published: 03 August 2022

Reviewing Editor: Fredrick Rosario Joseph, University of Colorado Anschutz Medical Campus, United States

culture generated using standard isolation protocols. This study will be valuable to scientists investigating the use of placental mesenchymal stromal cells in a therapeutic context.

Introduction

Mesenchymal stromal cells (MSCs) are a heterogeneous population of cells with secretory, immunomodulatory, and homing properties (***Viswanathan et al., 2019***). This population encompasses fibroblasts, myofibroblasts, pericytes, and tissue-specific progenitor populations. Traditionally researchers defined in vitro expanded MSCs by (1) plastic adherence, (2) expression of CD73, CD90, and CD105, lack of hematopoietic and endothelial marker expression (CD31, CD34, CD45, HLA-DR), and (3) the capacity to differentiate into adipocyte, chondrocyte and osteoblast lineages in vitro (***Dominici et al., 2006***). However, despite MSCs from different tissue sources (i.e. bone-marrow, adipose, umbilical cord, placenta) sharing expression of the minimal criteria antigens after in vitro culture, they functionally differ in a tissue-specific manner (***Du et al., 2016b***; ***Kozlowska et al., 2019***). This has been more recently acknowledged in a refined ISCT position statement that requires the tissue origin of MSCs to be provided along with evidence for their in vitro and in vivo functionality (***Viswanathan et al., 2019***).

It has become clear that in vitro culture may have significant impact on MSC phenotype, meaning that cultured MSCs may have a different phenotype from their in vivo/freshly isolated counterparts. For example, prior to culture adipose-derived MSCs are CD34+, whilst in vitro culture induces the loss of CD34 expression (***Lin et al., 2012***). The MSC-associated marker CD271 is also lost with plastic culture (***Brooks et al., 2020***), and MSC αSMA expression can be heavily impacted by culture media (***Boss et al., 2020***). Thus, the culture conditions used to expand MSCs can mask their true in vivo phenotype and heterogeneity. Furthermore, in any set of culture conditions the most competitive stromal cells will thrive and take over the culture, whilst other functionally diverse cells may be diluted out or lost. Understanding the true in vivo phenotype, and optimising culture conditions to minimize phenotypic 'drift' in vitro may enable researchers to better take advantage of the tissue specific properties of MSCs, and enable more accurate study of their roles in vivo.

Placental MSCs (pMSCs) are routinely isolated from the core of placental villi and propagated in culture (***Abumaree et al., 2013***; ***Castrechini et al., 2010***; ***Kusuma et al., 2018***). The placenta is a highly vascularised organ that develops rapidly over gestation in order to act as the conduit for nutrient and gas exchange between mother and fetus. pMSCs have been reported to reside in a perivascular niche where they can influence vascular development and function (***Castrechini et al., 2010***). In line with this, cultured pMSCs have well established angiogenic and haematopoietic paracrine effects in vitro and in vivo (***Chen et al., 2009***; ***Du et al., 2016a***). pMSCs are typically isolated by gross tissue culture methods (explant outgrowths or enzymatic digestion followed by plastic adherence), rather than by expression of specific cell surface markers (***Abumaree et al., 2013***; ***Pelekanos et al., 2016***). However, using gross digestion techniques it is impossible to determine the niche in which pMSCs reside. Previous work has assumed that in vitro pMSC expression of CD146, a marker with established perivascular expression in vivo, provides evidence of perivascular origins (***Castrechini et al., 2010***). However, work with bone marrow MSCs suggest CD146 expression is a tissue culture artefact (***Blocki et al., 2013***), and chipcytometry has localised in vitro MSC markers CD73, CD105 and CD90 outside of the perivascular niche in term placentae (***Consentius et al., 2018***). Together this sheds doubt on the perivascular origins of pMSCs, and highlights the need to better characterise their ex vivo phenotype in order to understand their functional role in vivo.

Our understanding of mesenchymal heterogeneity is expanding exponentially, and advances in single-cell technologies have uncovered a wide spectrum of mesenchymal and endothelial phenotypes with specific functions and spatial distributions (***Suryawanshi et al., 2018***; ***Takeda et al., 2019***; ***Vijay et al., 2019***). Mesenchymal heterogeneity can be used to spatially localise cells, identify cells involved in morphogenesis, angiogenesis or quiescence, and characterise inflammatory, anti-inflammatory, or invasive phenotypes (***Cimini and Kishore, 2021***; ***Mezawa et al., 2019***; ***Mezheyeuski et al., 2020***; ***Nazari et al., 2016***; ***Quintanilla et al., 2019***). Dramatic advances in flow cytometry over the past few decades have enabled the simultaneous quantification of upwards of 30 antigens, allowing detection of in depth cell heterogeneity. Whilst initiated in the haematopoietic field, the wealth of data produced using multicolour flow cytometry has driven the use of this technique for analysis of other cell types, including the mesenchymal lineages. To date the largest panel used to assess mesenchymal

cells (16-colours) was designed for analysis with conventional flow cytometry (***Brooks et al., 2020***). However, spectral flow cytometry has significant potential to further improve analysis of mesenchymal cells. The ability of spectral flow cytometry to measure a larger portion of the spectral signature of each fluorophore, and thus enable small differences between fluorophores to be discriminated, combined with the ability to remove autofluorescence (a prominent feature of mesenchymal cells) paves the way for assessing cells previously regarded as challenging for multicolour flow cytometry.

Here, we developed what to our knowledge is the largest multicolour spectral flow cytometry panel employed to date, in order to characterise the mesenchymal heterogeneity in first trimester placental tissue, and to ascertain the impact of in vitro MSC culture conditions on the subsequent phenotype of these populations.

Results

Design of a 23-colour flow cytometry panel to characterise the placental villous core

In order to investigate mesenchymal populations of the placental core a 23-colour flow cytometry panel (Panel One) was developed by starting from a 16-colour panel designed to investigate adipose-derived stromal vascular fraction on a conventional flow cytometer (BD FACS Aria II) (***Brooks et al., 2020***). The antigens included in this panel are based on the current literature surrounding the placenta, pMSCs, stromal/mesenchymal populations, endothelial progenitors and haematopoietic cells (***Table 1***).

Placental explants were dissected from the villous tissue and enzymatically digested to obtain a single cell suspension for flow cytometry (Figure 6). To enable us to focus on the mesenchymal core cells of interest, we needed to exclude trophoblasts (epithelial cells found in a bilayer on the outer edge of placental villi), endothelial cells, and hematopoietic cells. Whilst the initial enzymatic digestion removed the outer syncytiotrophoblast layer, inclusion of the cytotrophoblast maker β4 integrin in Panel One ensured any potential contaminating cytotrophoblasts directly beneath this were also excluded from analysis (***Table 1***, ***Figure 1B and C***). Endothelial cells were identified by expression of CD31 and CD144, specific expression of which is seen in blood vessels and early endothelial cell cords in first trimester placental villi (***Figure 1E***). The hematopoietic marker CD45 was used to exclude all cells of this lineage, while CD235a was used to identify and exclude red blood cells (***Table 1***). All remaining cells were considered to constitute the stromal fraction that makes up the mesenchymal core of the villi.

Full spectrum flow cytometry uncovers heterogeneous mesenchymal populations in the core of first trimester placental villi

First trimester placental villous explants were enzymatically digested to obtain a single-cell suspension that was stained with a master mix for Panel One and analysed on a Cytek Aurora. Due to the complexity of data obtained from a 23 colour panel, unbiased high-dimensional clustering of the data was undertaken using viSNE (Cytobank). viSNE enables visualization of high-dimensional single-cell data and is based on the t-Distributed Stochastic Neighbour Embedding (t-SNE) algorithm (***Amir et al., 2013***). To run the algorithm, debris, doublets, dead cells, β4 integrin +cytotrophoblasts and CD45+/CD235a hematopoietic cells were excluded by manual gating, then an equal number of cells from each villous core digest was selected using down-sampling (n=5) (***Figure 2***). Combining viSNE with known population marker expression, five distinct subsets were uncovered (***Figure 2***). Endothelial cells co-expressed CD31 and CD34 (Subset One) and made up 3.9% ± 2.5% of villous core cells (***Figure 3C and D***). $CD73^{+}CD90^{+}$ mesenchymal cells (Subset Two) made up 6.8% ± 9.7% of villous core cells on average, but decreased in abundance with increasing gestational age within the first trimester (***Figure 2C***). This gestational difference was confirmed by the inclusion of data from 22 additional first trimester villous core digests, analysed using a smaller panel targeted at cell sorting but containing the markers required to identify this population (***Figure 2D***). Together this data showed that at <10 weeks of gestation $CD73^{+}CD90^{+}$ cells constituted 14.02+8.84% of villous core cells, but significantly decreased to 0.77+0.83% of villous core cells at ≥10 weeks of gestation ($P<0.001$, n=27, placentae = 7–13.1 weeks of gestation) (***Figure 3C***). Perivascular cells (Subset Three) were identified by their expression of $CD146^{+}CD271^{+}$, and constituted 10.3% ± 4.7% of villous core cells (***Figure 3C***).

Table 1. Antigens included in Panel One and their functional roles with respect to the villous core.
Antigens are grouped by cell type (grey and white boxes).

Antigen	Full name/s	Functional capacity/relevance	References
ITGβ4/CD104	β4 integrin	Cell adhesion molecule that uniquely identifies cytotrophoblasts in the placenta.	***James et al., 2015***
CD45	Protein tyrosine phosphatase, receptor type, C. lymphocyte common antigen	Expressed on all nucleated haematopoietic cells.	***Hermiston et al., 2003***
HLA-DR	Human Leukocyte Antigen – DR isotype	Expressed by antigen presenting cells i.e. macrophages, MHC class II cell surface receptor, involved in antigen presentation and adaptive immunity,	***Cruz-Tapias et al., 2013***
CD235a/GPA	Glycophorin A	Red blood cell marker, identifies early emerging RBCs/erythroblasts from haemogenic endothelium	***Garcia-Alegria et al., 2018***; ***Mao et al., 2016***
CD41	Integrin alpha-IIb	Platelet marker. Expressed by earliest emerging haematopoietic cells from haemogenic endothelium	***Garcia-Alegria et al., 2018***; ***Li et al., 2005***
CD117/cKIT	Mast/stem cell growth factor receptor	Receptor expressed on haematopoietic stem cells and involved in their differentiation	***Rönnstrand, 2004***
CD144 /VE-cadherin	Vascular endothelial cadherin	Endothelial cell-cell adherens junctional marker, stabilises vessels, inhibits vascular growth, regulates vascular permeability.	***Giannotta et al., 2013***
CD34	Haematopoietic Progenitor Cell Antigen	Expressed by haematopoietic and vascular progenitors and adipose-derived MSCs. Transmembrane phosphoglycoprotein, thought to identify early placental progenitors	***Brooks et al., 2020***; ***Sidney et al., 2014***; ***Yoder, 2009***
CD31/PECAM1	Platelet endothelial cell adhesion molecule	Expressed by endothelial cells, platelets, macrophages and Kupffer cells, granulocytes, lymphocytes, megakaryocytes. Adhesion molecule found at endothelial intercellular junctions.	***Marelli-Berg et al., 2013***
VEGFR2/KDR	Vascular Endothelial Growth Factor Receptor 2/Kinase Insert Domain Receptor	Expressed by endothelial cells and thought to identify placental core progenitors. Receptor for angiogenic VEGF, involved in vasculogenesis and angiogenesis.	***Demir et al., 2007***
CD54/ICAM1	Intercellular Adhesion Molecule 1	Expressed at low levels on endothelial cells, monocytes and lymphocytes. Increased expression in response to inflammatory cytokines.	***Hubbard and Rothlein, 2000***
CD36/FAT	Platelet glycoprotein 4/ fatty acid translocase	Expressed by microvascular endothelial cells, and fibroblasts. Has an anti-angiogenic effect via binding Thrombospondin 1. Involved in fatty acid uptake.	***Dye et al., 2001***; ***Heinzelmann et al., 2018***; ***Silverstein and Febbraio, 2009***
CD90 /Thy-1	Thymocyte differentiation antigen 1	Expressed by MSCs, haematopoietic stem cells, fibroblasts, myofibroblasts.	***Viswanathan et al., 2019***
CD73 /NT5E	Ecto-5′-nucleotidase	Expressed by MSCs and endothelial cells. Works with CD39 to convert extracellular ATP to adenosine to create immunosuppressive effect.	***Roh et al., 2020***; ***Viswanathan et al., 2019***
CD39 /NTPDase	Ectonucleoside triphosphate diphosphohydrolase-1	Upregulated by MSCs to suppress lymphocyte activation. Immunosuppressive actions via the conversion of extracellular ATP (inflammatory) into adenosine (anti-inflammatory)	***Saldanha-Araujo et al., 2011***; ***Zhao et al., 2017***

Table 1 continued on next page

Table 1 continued

Antigen	Full name/s	Functional capacity/relevance	References
CD55/DAF	Decay-accelerating factor	Expressed by MSCs. Complement regulatory protein, inhibits C3 convertases thereby creating a threshold for complement activation, increased expression correlated with evasion of innate immune system	***Ruiz-Argüelles and Llorente, 2007***; ***Soland et al., 2013***
CD271 /NGFR / p75NTR	Low-affinity Nerve Growth Factor Receptor	Used in MSC and pericyte identification. Hypothesised to identify "stem-cell" or progenitor populations with superior differentiation and colony forming capacity.	***Barilani et al., 2018***; ***Kumar et al., 2017***
CD146/MCAM	Melanoma cell adhesion molecule	Adhesion molecule expressed by pericytes, endothelial cells and smooth muscle cells. Involved in the regulation of angiogenesis and vessel permeability.	***Crisan et al., 2009***; ***Leroyer et al., 2019***
CD248	Endosialin/ tumor endothelial marker 1	Pericyte and stromal cell marker. Involved in cell–cell adhesion, and host defence.	***Lax et al., 2010***; ***Tomkowicz et al., 2010***
CD142/TF	Tissue Factor/ thromboplastin	Expression correlated with pericytes, smooth muscle and fibroblasts. Activates blood clotting after injury, located outside the vasculature,	***Abe et al., 1999***; ***Morrissey, 2004***
CD26/DDP4	Dipeptidyl peptidase-4, adenosine deaminase complexing protein 2	Expressed by many tissues; T-cells, epithelial cells, ESCs, progenitor cells, placental myofibroblasts. Serine protease that cleaves a range of chemokines. Downregulation is correlated with increased stromal/myofibroblast proliferation.	***Kohnen et al., 1996***; ***Mezawa et al., 2019***; ***Ou et al., 2013***
PDPN	Podoplanin	Lymphatic vascular marker. Expression is correlated with increased fibroblast migration. Binds to CLEC-2 receptor on platelets.	***Astarita et al., 2012***; ***Suchanski et al., 2017***

Subset Four made up the largest proportion of mesenchymal cells in the core (47.8+17.0%) and were identified by co-expression of podoplanin^{+}CD36^{+} (***Figure 3C***). The remaining cells, expressing only the myofibroblast-associated markers CD26^{+}CD90^{+}, were classified as Subset Five and constituted 31.3% ± 12.6% of villous core cells. Subset Five were negative for all other markers investigated, suggesting they are more differentiated myofibroblast-like cells (***Figure 3C***).

Mesenchymal subsets have distinct phenotypes indicating functionally diverse roles in the villus core

In order to consider what the different subsets functionally represent within the core of placental villi, we further interrogated their phenotype and proportional contribution to the villus core, with consideration to which subset phenotypes pMSCs may originate from. CD73^{+}CD90^{+} cells (Subset Two) were the only villous population to co-express CD90 and CD73, both MSC-associated markers. This subset also expressed podoplanin (correlated with increased migratory capacity), low levels of CD142 (involved in blood coagulation [***Morrissey, 2004***]), and had heterogeneous expression of CD146 and CD271 (perivascular associated markers) (***Figure 3B***). A lack of CD26 (associated with myofibroblasts and cell proliferation) made this population distinct from the other perivascular and mesenchymal cell populations identified in the villous core using Panel One.

Perivascular cells (Subset Three), identified by expression of CD271 or CD146, did not co-express CD73, CD142 or podoplanin. However, they did express CD26 and CD90, and in line with this they co-localised with Subset Five (also CD26^{+}CD90^{+}) on the viSNE plot (***Figure 3B***). The phenotype of CD271^{+}CD146^{+} cells was relatively conserved between placentae with some inter-placental variance in CD271, CD36 and CD90 expression (***Figure 3B***).

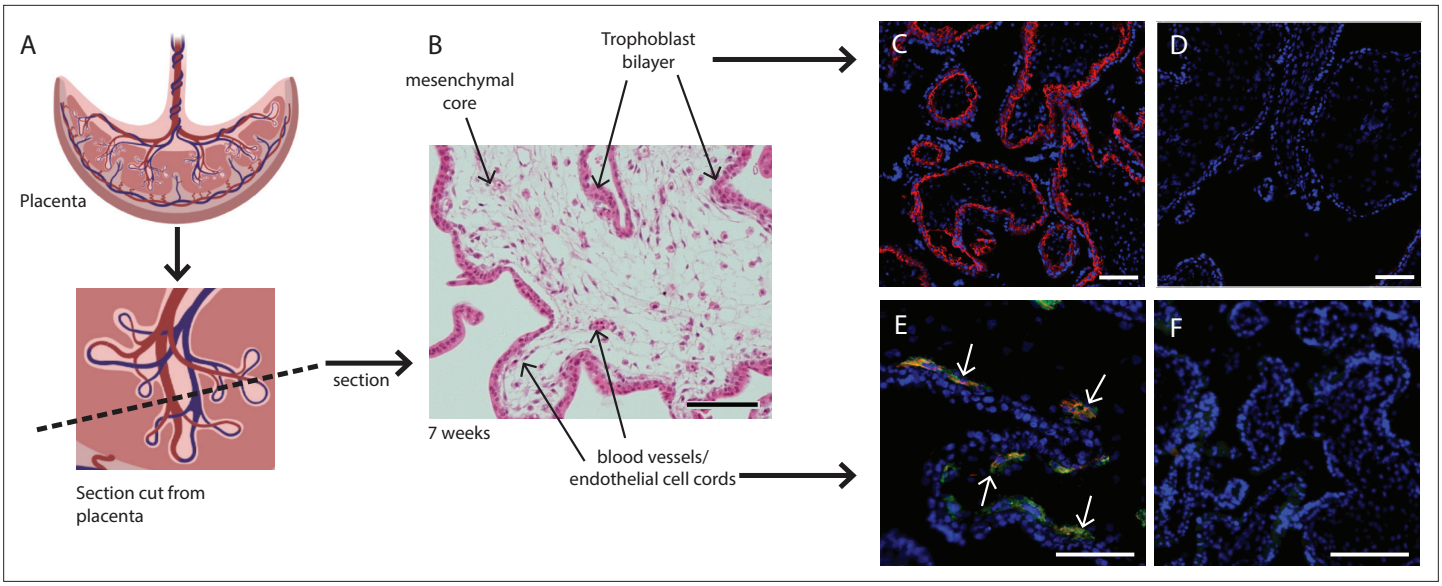

Figure 1. Placental villus structure and specificity of markers used to exclude unwanted cell populations. (**A**) Placental villous morphology and plane of section, (**B**) haematoxylin and eosin staining of a thin section though a placental villus (7.1 weeks), localisation of (C) β4 integrin (red) to cytotrophoblasts and (E) CD144 (red) and CD31 (green) to blood vessels (white arrows) in placental villus sections confirmed antibody specificity. No fluorescence is seen in negative IgG controls (**D, F**) run simultaneously. Nuclei are counterstained with DAPI (blue). Scale bar = 100 μm. Rendered images in (A) have been acquired from Biorender.com.

Subset Four was identified by expression of podoplanin and CD36, and co-expressed CD26, CD90, and CD142, but was negative for the MSC-associated marker CD73 (***Figure 3B***). As the largest population within the villous core and expressing proliferative/migratory associated markers (CD26, podoplanin [***Suchanski et al., 2017***]) this subset was considered the most likely in vivo candidate to contribute to pMSCs that are derived in explant derived cultures.

Phenotypically divergent mesenchymal stromal cell populations converge after in vitro culture

In order to investigate the origins of in vitro cultured pMSCs in relation to the subsets identified with Panel One we used fluorescence activated cell sorting (FACS) to isolate subsets of interest from first trimester villous digests and assessed their phenotype in relation to cultured pMSCs obtained using an explant outgrowth method. Here we focussed on two ex vivo cell populations; $CD73^{+}CD90^{+}$ cells (Subset Two) as the only population to phenotypically align with the ISCT marker criteria for MSCs (***Dominici et al., 2006***), and $podoplanin^{+}CD36^{+}$ cells (Subset Four), which expressed markers of proliferative/migratory cells (characteristics associated with pMSCs). Following sorting, cells were cultured for 7 days in EGM-2 previously demonstrated to sustain fetal-derived pMSCs (***Boss et al., 2020***; ***Figure 4***). In culture, both populations underwent phenotypic convergence, forming cells with a mesenchymal-like morphology, that were $CD90^{+}CD73^{+}CD142^{+}CD271^{-}CD36^{-}$ at day 7 of culture (***Figure 4B and C*** and ***Figure 4—figure supplement 1***).

Despite this overall convergence, differences between the two populations did remain. The proliferation/myofibroblast associated marker CD26 was only expressed by a small proportion of $CD73^{+}CD90^{+}$ cells at the time of isolation and although the percentage of $CD26^{+}$ cells increased over time in culture, most cells remained negative suggesting this marker was not upregulated with the culture conditions used here. Conversely, all $podoplanin^{+}CD36^{+}$ cells were $CD26^{+}$ at isolation and remained $CD26^{+}$ after culture. Although CD146, was used to identify perivascular cells in the placenta (***Castrechini et al., 2010***), was not assessed on cells during isolation (this marker was not contained in Panel Two), phenotyping experiments with Panel One demonstrated that a subpopulation of $CD73^{+}CD90^{+}$ cells expressed CD146 (5.89+5.82%) and therefore, could be perivascular. Whereas, $podoplanin^{+}CD36^{+}$ cells were negative for CD146. After 7 days culture this $CD146^{+}$ subpopulation was still present in $CD73^{+}CD90^{+}$ cells (15.55+6.87%). However, all $podoplanin^{+}CD36^{+}$ cells expressed

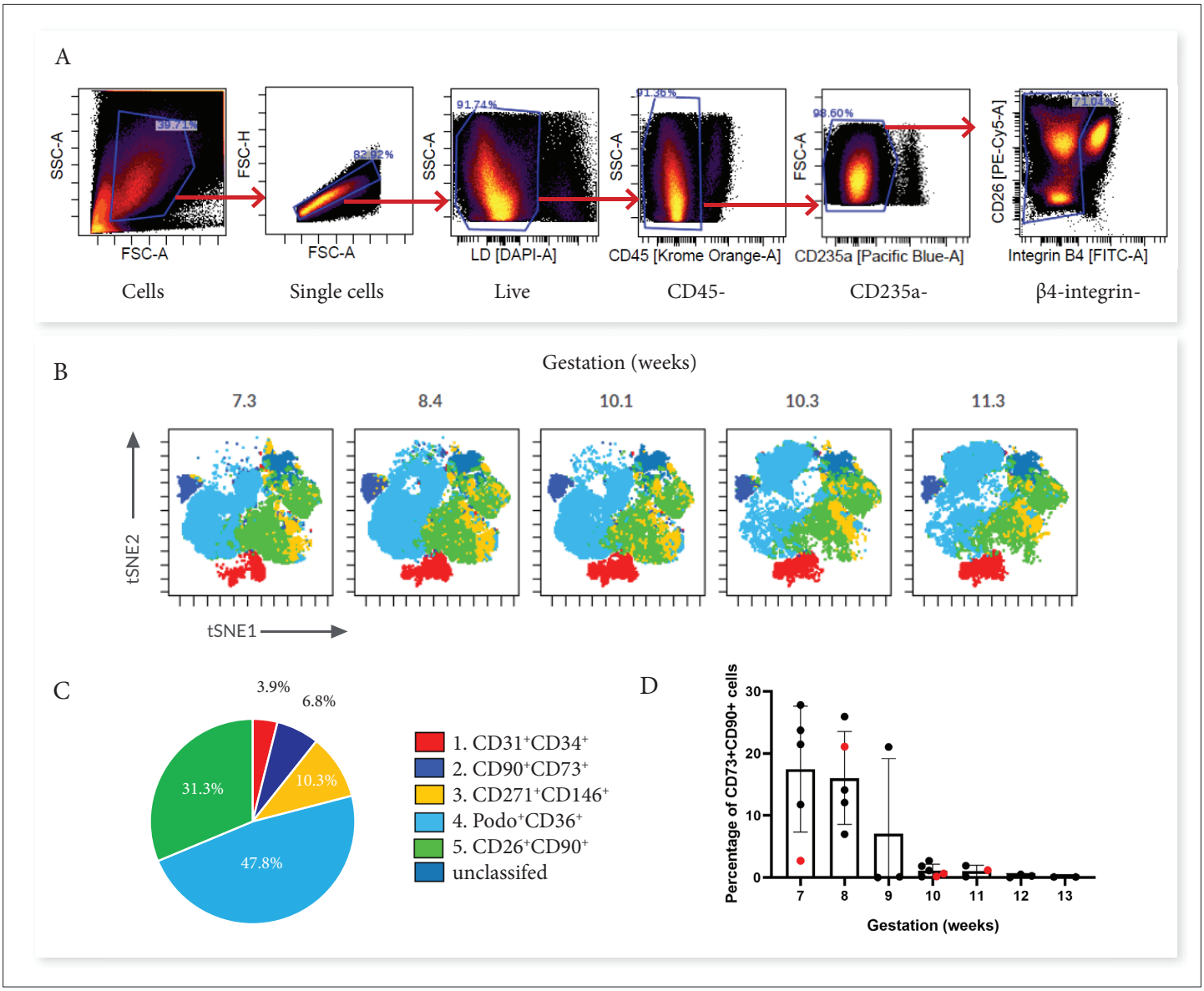

Figure 2. Categorisation of placental villus core subsets using Panel One markers. (**A**) Samples were gated to exclude debris, doublets, dead cells, hematopoietic cells (CD45$^+$ and CD235a$^+$), and cytotrophoblasts (β4 integrin). (**B**) Marker expression was used to categorise five subsets that were overlaid onto viSNE plots generated in Cytobank. (**C**) The average percentage contribution of each subset is presented as a pie chart. (**D**) A scatter plot with bars depicting the mean percentage of CD73$^+$CD90$^+$ cells from villous core cells across first trimester analysed on an Aria II (n=24, black) or an Aurora spectral analyser (n=5, red). Error bars represent the standard deviation of the mean.

CD146 after seven days in culture, demonstrating differential response of these subsets to the in vitro culture conditions (***Figure 4D and E***, and ***Figure 4—figure supplements 1 and 2***).

In order to determine whether cultured pMSCs are likely to be made up of CD73$^+$CD90$^+$ or podoplanin$^+$CD36$^+$ populations, we simultaneously characterised explant isolated pMSCs that had been generated and cultured in the same medium (EGM-2) (n=3, p2-6). This demonstrated that pMSCs were CD90$^{low/neg}$CD73$^+$CD26$^+$CD142$^+$CD146$^+$podo$^+$CD34$^-$CD271$^-$CD36$^-$(***Figure 4F*** and ***Figure 4—figure supplements 1 and 2***), more closely aligning with the phenotype of cultured podoplanin$^+$CD36$^+$ cells (Subset Four).

In previous work we have demonstrated that pMSCs upregulate the contractile markers αSMA and calponin when transferred from EGM-2 to standard MSC medium (advanced-DMEM/F12) (***Boss et al., 2020***). In order to investigate whether CD73$^+$CD90$^+$ cells (Subset Two) or podoplanin$^+$CD36$^+$ cells (Subset Four) could similarly upregulate contractile markers, after 7 days in EGM-2 the medium was changed

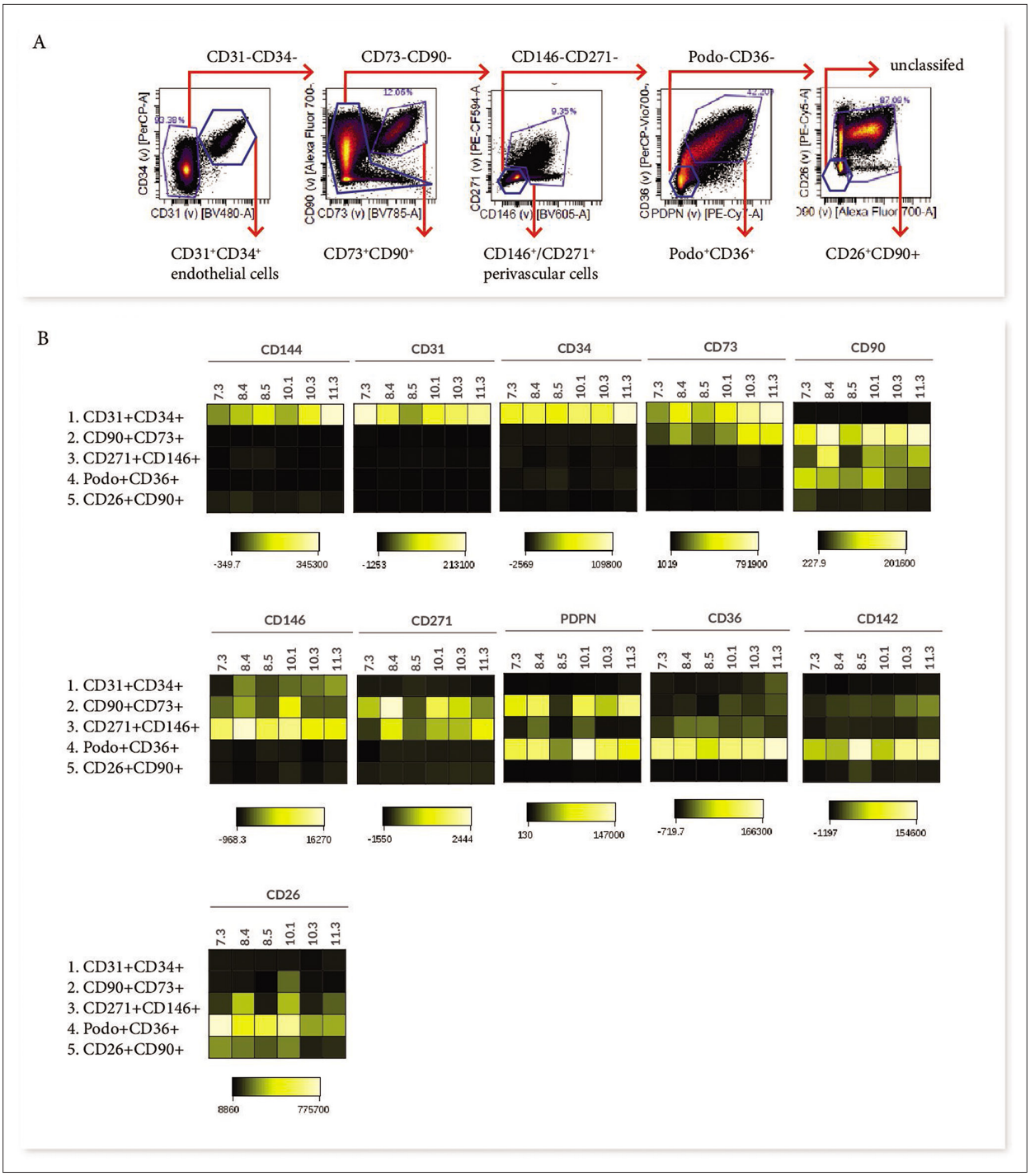

Figure 3. Phenotypic characterisation of villous core subsets. (**A**) The gating strategy used to identify subsets (CD31⁺CD34⁺, CD73⁺CD90⁺, perivascular cells, podoplanin⁺CD36⁺ and CD26⁺CD90⁺), and (B) heat maps comparing the expression of specific antigens between subsets (n=5).

to advanced-DMEM/F12. Whilst in EGM-2 very few cells in either population expressed αSMA and no cells expressed calponin, in advanced-DMEM/F12, both populations upregulated both of these markers (***Figure 5***). Expression of the more mature smooth muscle marker MYH-11 was not observed in either CD73⁺CD90⁺ or podoplanin⁺CD36⁺ cells cultured in either EGM-2 or advanced DMEM/F12 (***Figure 5***).

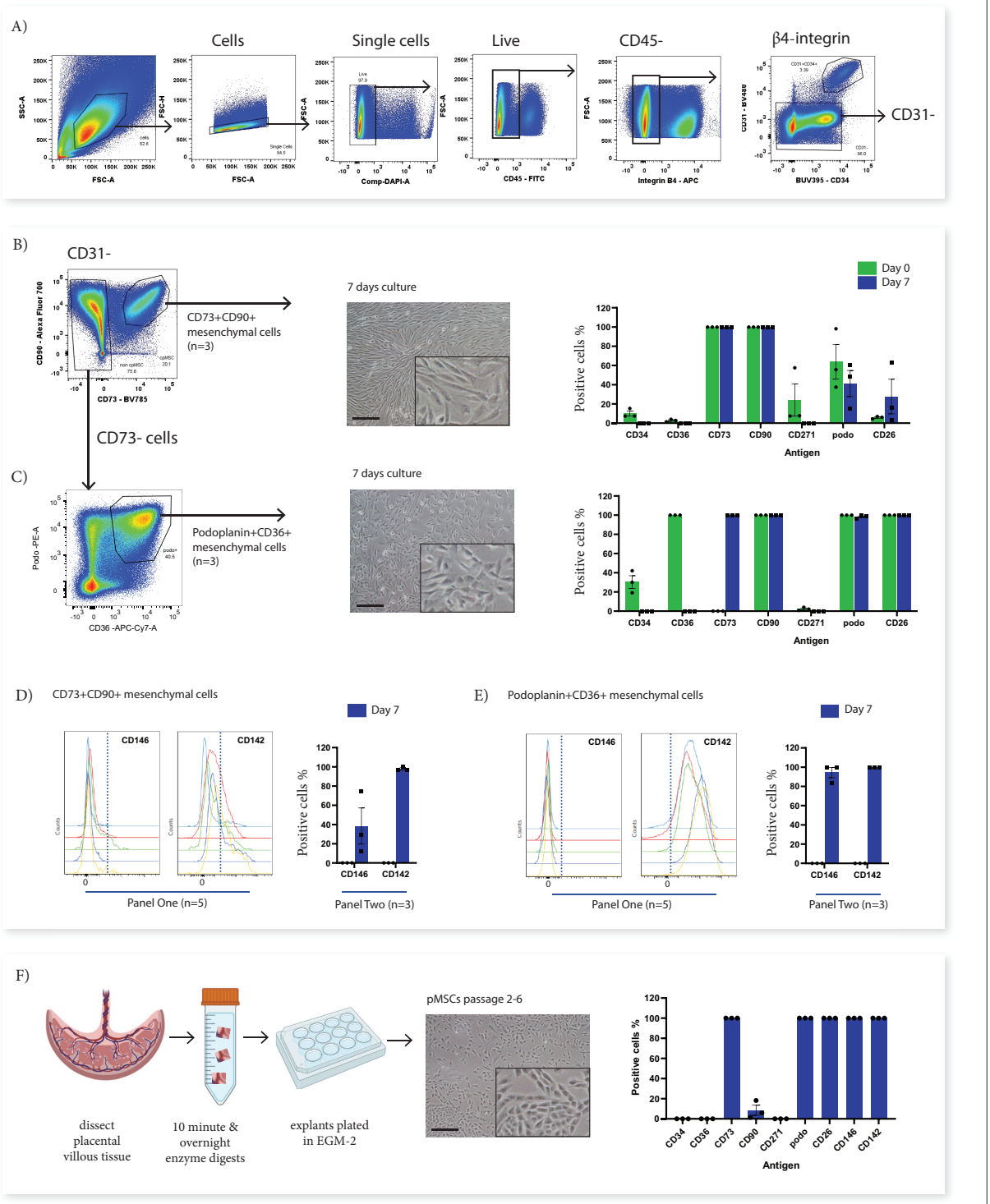

Figure 4. In vitro culture of CD73$^+$CD90$^+$ and podoplanin$^+$CD36$^+$ cells. (**A**) FACS sorting was used to isolate CD73$^+$CD90$^+$ and podoplanin$^+$CD36$^+$ cells from placental villous core cells (n=3). (**B**) Morphology and phenotype of CD73$^+$CD90$^+$ cells after 7 days in culture. (**C**) Phenotype of podoplanin$^+$CD36$^+$ cells after 7 days in culture. (**D**) CD146 and CD142 expression on CD73$^+$CD90$^+$ analysed with Panel One (day 0, n=5) or at 7 days after culture (n=3).

Figure 4 continued on next page

Figure 4 continued

(**E**) CD146 and CD142 expression on podoplanin$^+$CD36$^+$ cells analysed with Panel One (day 0, n=5) or at 7 days after culture (n=3). (**F**) Isolation of explant-derived pMSCs, and morphology and phenotype of passaged pMSCs (n=3). Error bars = standard error of the mean and scale bar = 100 µm.

The online version of this article includes the following figure supplement(s) for figure 4:

Figure supplement 1. Representative 2-dimensional flow cytometry plots displaying the phenotype of FACS sorted CD73$^+$CD90$^+$ and podoplanin$^+$CD36$^+$ cells after 7 days culture in vitro (n=3), and explant isolated pMSCs after culture in vitro (n=3, p2-6).

Figure supplement 2. Flow cytometry histograms displaying the phenotype of FACS sorted CD73$^+$CD90$^+$ and podoplanin$^+$CD36$^+$ cells after 7 days culture in vitro (n=3), and explant isolated pMSCs after culture in vitro (n=3, p2-6).

Discussion

Common sources of MSCs used in clinical trials include; uncharacterised adipose, bone-marrow, and placental stroma. Identifying functionally different mesenchymal cells and defining the origins for tissue-specific MSCs could improve these applications. Here, we used a high-dimensional flow cytometry panel to uncover at least four different mesenchymal populations with distinct expression profiles in the villous core of first trimester placentae, indicating the presence of functionally specialised cells. This mesenchymal heterogeneity could translate to different physiological capabilities important for clinical therapies and aid understanding of the role of these cells in vivo.

Characterising the villous core populations allows us to better understand how the placenta functions and develops, and enables targeting of populations for functional analysis. From the four mesenchymal populations classified in this work three populations, perivascular cells (Subset Three), podoplanin$^+$CD36$^+$ cells (Subset Four), and CD26$^+$CD90$^+$ myofibroblasts (Subset Five) all closely aligned with populations described in prior single-cell RNA sequencing data from first trimester placentae (***Suryawanshi et al., 2018***). However, this single-cell RNA sequencing dataset did not report a population that aligned with CD73$^+$CD90$^+$ cells (Subset Two), instead reporting that only endothelial cells expressed CD73 in the placental core. The ability to assess larger cell numbers by flow cytometry in our work, and the low abundance of CD73$^+$CD90$^+$ cells after 9 weeks of gestation, means that this population may not have been detected as a distinct population by single cell RNA-seq. Furthermore, RNA expression does not always accurately reflect protein expression (***Reimegård et al., 2021***). This highlights the importance of protein level characterisation of cells from fresh tissue, and the ability of multicolour flow cytometry to undertake this at single cell resolution complements and builds on single cell gene expression datasets.

The first major aspect of this work to consider is what each subset could represent and what its phenotype reflects. CD73$^+$CD90$^+$ cells were unique from the other mesenchymal populations and could be identified by their expression of CD73, which was shared only with endothelial cells. The abundance of this population at <10 weeks of gestation hints at their involvement in processes that occur early in gestation such as vasculogenesis or haematopoiesis. CD73$^+$CD90$^+$ cells co-expressed podoplanin, but were distinct from other mesenchymal subsets in that they did not express CD26. This combined expression pattern alludes to two potential functional roles of these cells in the placenta. First, expression of podoplanin and low expression of CD26 are both associated with a migratory/invasive phenotype (***Mezawa et al., 2019***; ***Ward et al., 2019***). As the decline in abundance of these cells after 9 weeks of gestation corresponds to the regression of villi and blood vessels from the distal side of the gestational sac (***Burton and Jauniaux, 2018***), this raises the possibility that CD73$^+$CD90$^+$ cells could be involved in this regression of the villi, or they arise transiently as the result of an early endothelial to mesenchymal transition in the placenta whereby, endothelial cells involved in vascular regression lose their junctional markers and gain a mesenchymal/migratory phenotype (***Pinto et al., 2016***). Secondly, expression of podoplanin and a lack of CD26 expression on CD73$^+$CD90$^+$ cells indicates potential roles in haematopoiesis. Several studies have demonstrated that inhibiting CD26 enhances homing, engraftment and differentiation of hematopoietic stem cells (***Christopherson et al., 2004***; ***Kawai et al., 2007***), and thus a lack of CD26 expression on CD73$^+$CD90$^+$ cells could suggest they are involved in blood lineage migration/differentiation as both Hofbauer cells (placental macrophages) and nucleated red blood cells are found in the villous stroma in the first trimester (***Van Handel et al., 2007***). Furthermore, podoplanin identifies connective stroma in lymphoid organs that produces a network of collagen-rich fibres to enable movement of lymphocytes via interactions with leukocyte CLEC-2 receptors (***Link et al., 2011***; ***Nazari et al., 2016***; ***Onak Kandemir et al., 2019***;

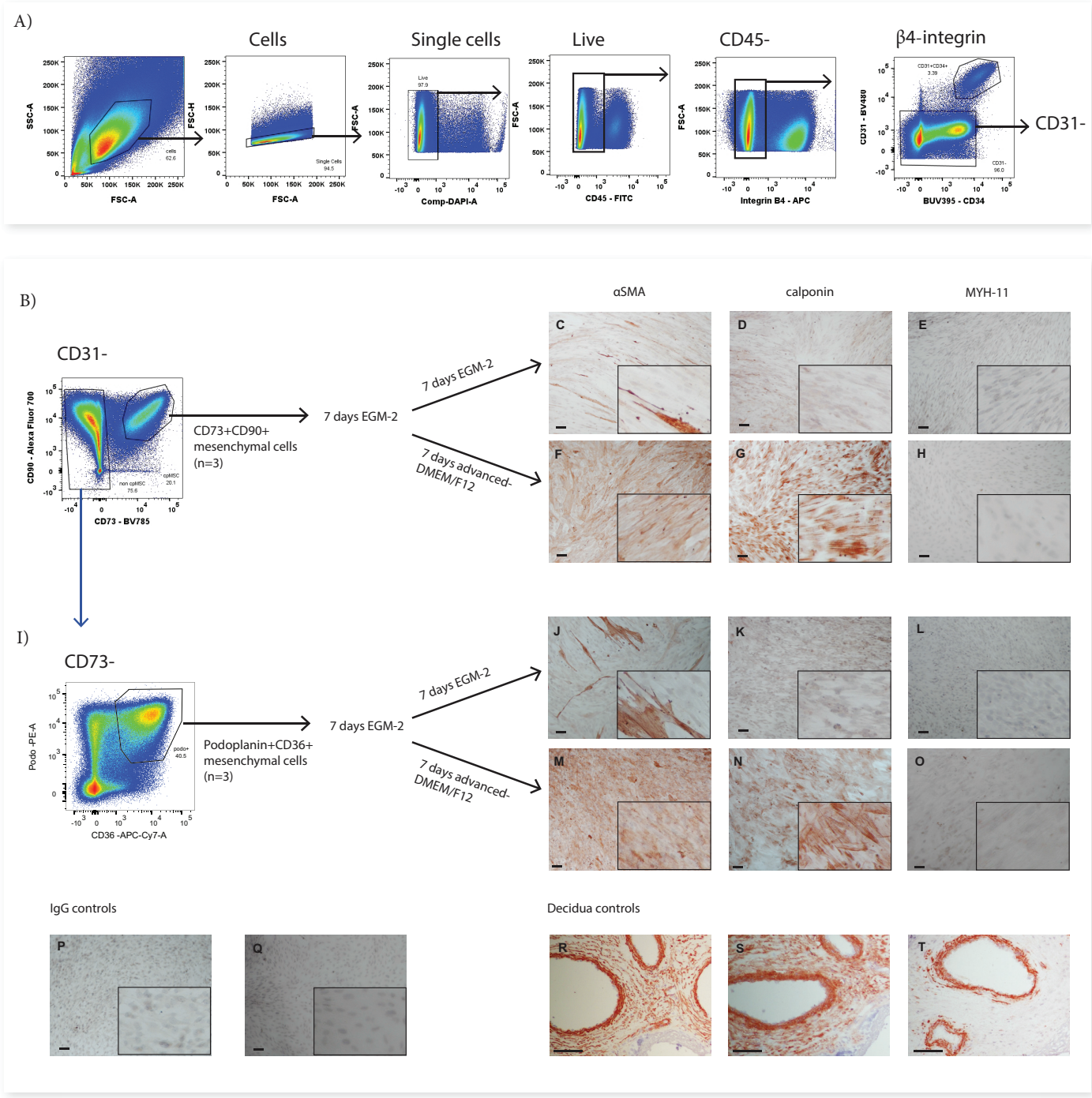

Figure 5. CD73$^+$CD90$^+$ and podoplanin$^+$CD36$^+$ cells upregulate markers consistent with contractile cells. (**A**) FACS sorting was used to isolate CD73$^+$CD90$^+$ and podoplanin$^+$CD36$^+$ cells from placental villous core digests (n=3). CD73$^+$CD90$^+$ (**B**) and podoplanin$^+$CD36$^+$ (**I**) cell expression of αSMA (**C, F, J, M**), calponin (**D, G, K, H**) or MYH-11 (**E, H, L, O**) following 7 days of culture in advanced-DMEM/F12 or EGM-2. Irrelevant mouse IgG (**P**) and rabbit IgG (**Q**) were used as negative controls. Decidual sections containing spiral arteries with intact smooth muscle layers were used as positive controls for staining (**R–T**). Scale bar = 100 μm.

Wang et al., 2011). The stroma of early placental villi is poorly vascularised therefore podoplanin$^+$ cells could enable blood lineage cells (including Hofbauer cells) to migrate throughout the villous core (***Ingman et al., 2010***). Indeed, Hofbauer cells have been co-localised with podoplanin expressing stroma in term placentae (***Onak Kandemir et al., 2019***). Together this suggests CD73$^+$CD90$^+$ cells

may represent a functionally divergent population, that is abundant in the early first trimester placenta which is specialised to facilitate/promote hematopoietic migration and differentiation, and morphogenesis of the placenta during regression of the distal villi.

The largest subset identified, podoplanin^{+}CD36^{+} cells (Subset Four) was hypothesised to constitute the majority of connective villous stroma and play an important role in villous stroma expansion. Similar to CD73^{+}CD90^{+} cells, the expression of podoplanin in this population suggests they may play a role in facilitating hematopoietic transport throughout the poorly vascularised first trimester stroma, and may have a migratory phenotype. However, podoplanin^{+}CD36^{+} cells had a high expression of CD26 which identifies fibroblasts involved in wound healing/fibrosis and the associated extracellular matrix deposition (**Soare et al., 2020**; **Worthen et al., 2020**) suggesting an alternative or additional role in villous expansion and growth. The corresponding podoplanin^{+}CD36^{+} population observed in the prior single cell RNA-seq dataset, expressed genes associated with angiogenesis (*IL6, ANGPTL-4, TNFAIP6*), suggesting they may also provide a paracrine stimulus for placental vascular development which is undergoing vasculogenesis and angiogenesis over first trimester (**Chang et al., 2012**; **Hato et al., 2008**; **Suryawanshi et al., 2018**).

Perivascular cells (Subset Three) were identified by their expression of either CD271 or CD146, both markers that localise in a perivascular niche (**Castrechini et al., 2010**; **Lv et al., 2014**). CD26^{+}CD90^{+} myofibroblasts (Subset Five) were negative for all other markers in Panel One and therefore, were hypothesised to represent contractile/less proliferative myofibroblasts. Indeed, prior single-cell RNA sequencing work identified that populations aligning with perivascular cells and CD26^{+}CD90^{+} myofibroblasts reported here had a respectively low or high expression of markers associated with contractile myofibroblasts and mature perivascular cells (*ACTA2* (αSMA) and *CNN1* (calponin)) (**Kumar et al., 2017**; **Suryawanshi et al., 2018**). The lower expression of contractile markers in perivascular cells in comparison to CD26^{+}CD90^{+} myofibroblasts may initially appear unexpected, but as the first trimester placental vasculature is relatively immature it would not necessarily be expected that perivascular cells had high expression of contractile markers at this stage of gestation (**Zhang et al., 2002**). Interestingly, our in vitro experiments demonstrated that both CD73^{+}CD90^{+} cells (Subset Two) and podoplanin^{+}CD36^{+} cells (Subset Four) upregulated αSMA and calponin when transferred from EGM-2 to advanced-DMEM/F12, paralleling the upregulation observed in explant-isolated first trimester pMSCs when cultured in this medium (**Boss et al., 2020**). The in vivo niche that CD73^{+}CD90^{+} cells and podoplanin^{+}CD36^{+} cells reside in could determine whether differentiated cells contribute to perivascular or myofibroblast contractile cells and more specific markers may be required to tease apart these differences. Indeed, in term placentae contractile perivascular cells express both αSMA and calponin, but extravascular αSMA^{+} cells are also present and thought to allow stem villi to contract and expand in volume (**Dellschaft et al., 2020**; **Farley et al., 2004**).

Cultured MSCs are often described as homogeneous. However, there is strong evidence that MSCs upregulate/downregulate markers in response to in vitro culture conditions, and underlying functional and phenotypic heterogeneity could be missed (**Blocki et al., 2013**; **Boss et al., 2020**; **da Silva Meirelles et al., 2015**). In the MSC field, CD73 is thought to be ubiquitously expressed by MSCs (**Dominici et al., 2006**). However, that podoplanin^{+}CD36^{+} cells upregulate CD73 expression after culture demonstrates expression of this marker may also be a culture artefact. The phenotypic convergence of different mesenchymal populations was further demonstrated by the loss of CD36 and CD271 expression, from podoplanin^{+}CD36^{+} and CD73^{+}CD90^{+} cells respectively, additional markers that made these populations distinct ex vivo. However, expression of CD26 was unaffected by culture, and CD146 was differentiability affected by culture in the two populations. This demonstrates that the nuances of culture adaptation are cell-specific as much as they may be media-specific.

Changes to "MSC" phenotype do not necessarily reflect gain/loss in function. For example bone-marrow MSCs isolated by their expression of CD146 stabilize endothelial tube formation in vitro, whereas, CD146^{-} MSCs, that subsequently upregulate CD146 in vitro, are unable to stablise tube formation (**Blocki et al., 2013**). Thus, ex vivo phenotype may be a more accurate indicator of a cells' functional capacity and highlights the importance of characterizing mesenchymal cells prior to culture. The four placental mesenchymal populations identified here are likely to play different roles in the placenta, and therefore have different functional and therapeutic capacities. pMSCs are often acquired by macerating the villous tissue in order to obtain a single cell suspension that is plated in plastic tissue culture flasks (**Papait et al., 2020**; **Pelekanos et al., 2016**). Thus all of the populations

identified in this work could be present within such single cell suspensions. However, the population/s with a competitive advantage in culture, either as a result of the culture conditions employed, or as a result of the isolation process itself (enzymes involved, explant-based, plated suspension, enriched for expression of a marker), are likely to outcompete and become the dominant cell in culture. Indeed, our group has demonstrated that under different media conditions fetal pMSCs rather than maternal cells are enriched in culture in EGM-2 (***Boss et al., 2020***). Characterising the explant isolated pMSCs in more depth in this work demonstrated they express podoplanin, CD26, and CD142, making their origins more likely to be podoplanin^{+}CD36^{+} (Subset Four) rather than CD73^{+}CD90^{+} cells (Subset Two), perivascular cells (Subset Three) or CD26^{+}CD90^{+} myofibroblasts (Subset Five). The heterogeneity identified in this work creates an opportunity to select subsets of these mesenchymal cells more suited to specific uses i.e. with anti-inflammatory/immunomodulatory or angiogenic capacity, and to target media conditions that maintain or transform their in vivo phenotype and desired properties. Furthermore, separately culturing these different subsets will allow us to better to understand their functional contributions to placental development, and whether in vitro culture conditions that promote surface marker convergence also result in functional convergence.

Finally, it is important to consider potential limitations of the use of the cell types identified in therapeutic applications, for example the potential pro-coagulant role of cell surface expression of CD142 (Subset Four) (***Moll et al., 2020***), or the prior association of CD36 expression (seen on Subset Four) with adipose progenitors, raising the possibility that these cells could be prone to differentiating down this pathway in vivo (***Gao et al., 2017***; ***Hanschkow et al., 2022***). Conversely, the expression of podoplanin (Subset Two and Four), may indicate an increased migratory capacity, which could potentially enhance migration to sites of therapeutic interest when administered in vivo (***Ward et al., 2019***). Future work to understand the in vivo and ex vivo functional capacity of each subset identified will help elucidate both their role in placental physiology, and inform potential downstream applications of these cells or their counterparts that may be present in term placentae (a more accessible source of placental cells for therapeutic applications).

In conclusion, this work has demonstrated how simplistic post-culture MSC phenotyping will fail to detect the abundant mesenchymal heterogeneity that exists within the placenta. The phenotypic heterogeneity uncovered in first trimester placental mesenchymal cells indicates their potentially diverse functional roles and highlights the crucial need to thoroughly characterise mesenchymal cells that are used in functional assays or in a therapeutic capacity. The success of this multicolour flow cytometry panel in uncovering mesenchymal cell heterogeneity paves the way for other panels assessing mesenchymal and vascularised tissues. Panels like this could be used to assess cellular dysfunction in pathologies such as cancer, cardiovascular disease and infection, as well as to interrogate different tissues in order to better understand cell function. Identifying the pathological phenotype of mesenchymal/vascular cells in pathologies could lead to therapeutic targets. Indeed, in the context of pregnancy, emerging data has suggested that MSC function is altered in the pregnancy complication fetal growth restriction, with potential impacts on placental vascular function (***Boss et al., 2021***; ***Gillmore et al., 2022***). Thus, this flow cytometry antibody panel, optimised for placental cells, combined with assessment of different stromal subsets identified in this work, could provide an important tool to better understand normal and abnormal placental development and function across gestation.

Table 2. Primary conjugated antibodies used to confirm specificity of cytotrophoblast or endothelial markers.

Antigen	Fluorophore	Clone	Dilution	Supplier
β4 integrin	FITC/APC	450-9D	1:200	Thermofisher
CD144	BV421	55–7 H1	1:200	BD
CD31	BV480	WM59	1:200	BD

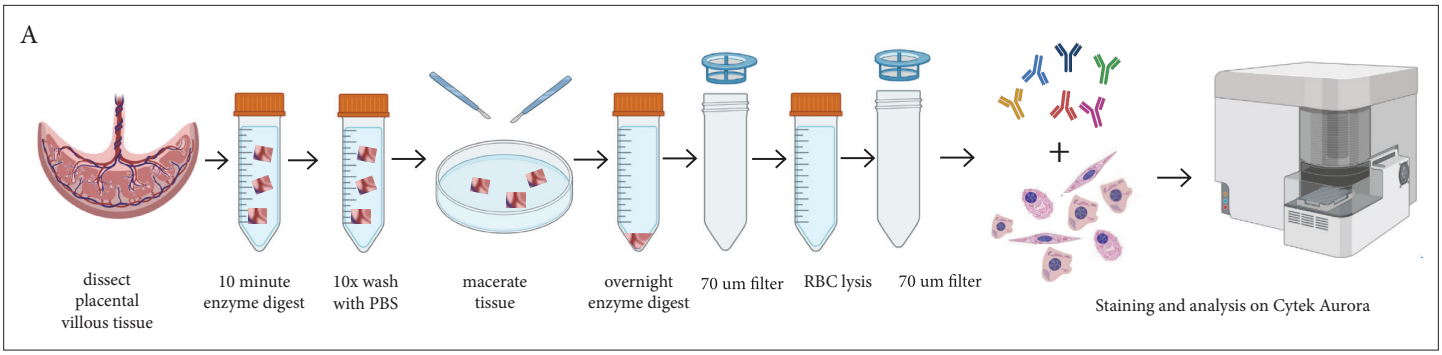

Figure 6. Schematic diagram demonstrating the enzymatic digestion process used to obtain a single-cell suspension of placental villous core cells for flow cytometry analysis.

Materials and methods

Immunohistochemistry

All placentae used in this work were collected following informed consent with approval from the Northern X Health and Disability Ethics Committee (NTX/12/06/057/AM09). First trimester placental villous tissue (7–10 weeks of gestation) was snap-frozen in OCT compound (VWR) and 5 µm cryosections of tissue were cut and fixed in ice-cold acetone for 5 minutes. Sections were blocked with Fc Blocking Reagent (Miltenyi Biotech) for 30 minutes, then incubated with primary antibodies for 1 hour (***Table 2***). β4 integrin and CD31 were visualised by their directly conjugated fluorophores (***Table 2***). CD144-BV421 was visualised by the addition of Biotin-SP AffiniPure Goat Anti-Mouse IgG (1 µg/mL) (Jackson Lab, JI115065166) for 1 hr, washing in PBS-tween, and then the addition of Streptavidin Alexa Fluor 594 (0.5µg/mL, Invitrogen) for 30 minutes. Nuclei were visualised by counterstaining with DAPI (2 µg/ml) for 5 minutes. Sections were mounted using Citifluor AF1 (Agar Scientific), and imaged on an inverted Zeiss Axioplan 2 fluorescent microscope (Zeiss).

Isolation of placental villous core cells for ex vivo phenotyping

In order to assess placental villous core cells we modified the protocol developed by ***Pelekanos et al., 2016***; ***Figure 6***. In brief, villous tissue was carefully dissected away from the fetal membranes and washed thoroughly in PBS to remove maternal blood and debris. Placental explants (~1 cm^2) were denuded of trophoblasts (the epithelial cells that are present around the outside of placental villi) by digestion in 10 mL/1 g tissue of Enzyme Digest Solution (1 mg/mL Dispase II, 0.5 mg/mL Collagenase A and 1.5 mg/mL DNAse I (Sigma-Aldrich, USA)) in advanced-DMEM/F12 (Thermofisher) for ten minutes at 37 °C as previously described (***Boss et al., 2020***). Explants were then washed repeatedly (at least 10 times) in PBS, until cellular material is no longer released. Washed explants were then placed in a 90 mm Falcon petri dish (Corning, US) and finely macerated with two sterile disposable scalpels (Swann Morton No.20, England). The tissue was transferred to a 50 mL Falcon tube (Corning, China) with 10 mL of Enzyme Digest Solution. The Falcon tube was briefly vortexed and then placed onto a rocker at room temperature overnight. The next morning the Falcon tube containing the digested villous tissue and enzyme solution was diluted with 40 mL PBS and filtered through a 70 µm filter. The filtrate containing villous core cells was centrifuged at 220xg for five minutes, and the supernatant was removed. 10 mL of 1 x RBC Lysis Buffer (Biolegend, USA) was incubated with the cell suspension for ten minutes to remove unwanted RBCs. Remaining cells were centrifuged at 220xg for five minutes and supernatant removed prior to flow cytometry.

Large amounts of syncytiotrophoblast fragments are released during the washing stages of the first digest, and based on our experience with similar villous digest protocols (***James et al., 2015***) it is likely that the majority of the syncytiotrophoblast is removed at this stage. Remaining large fragments of syncytiotrophoblast would be removed by the 70 µm cell strainers during the digestion process, whilst smaller syncytiotrophoblast fragments would not have an intact cell membrane, and thus nuclei would stain positive for DAPI and be gated out from analysis and/or downstream cell sorting. Whilst the villous core digest protocol would also be expected to remove the vast majority of extravillous trophoblasts, to quantify the degree of potential contamination of this cell type we stained villous

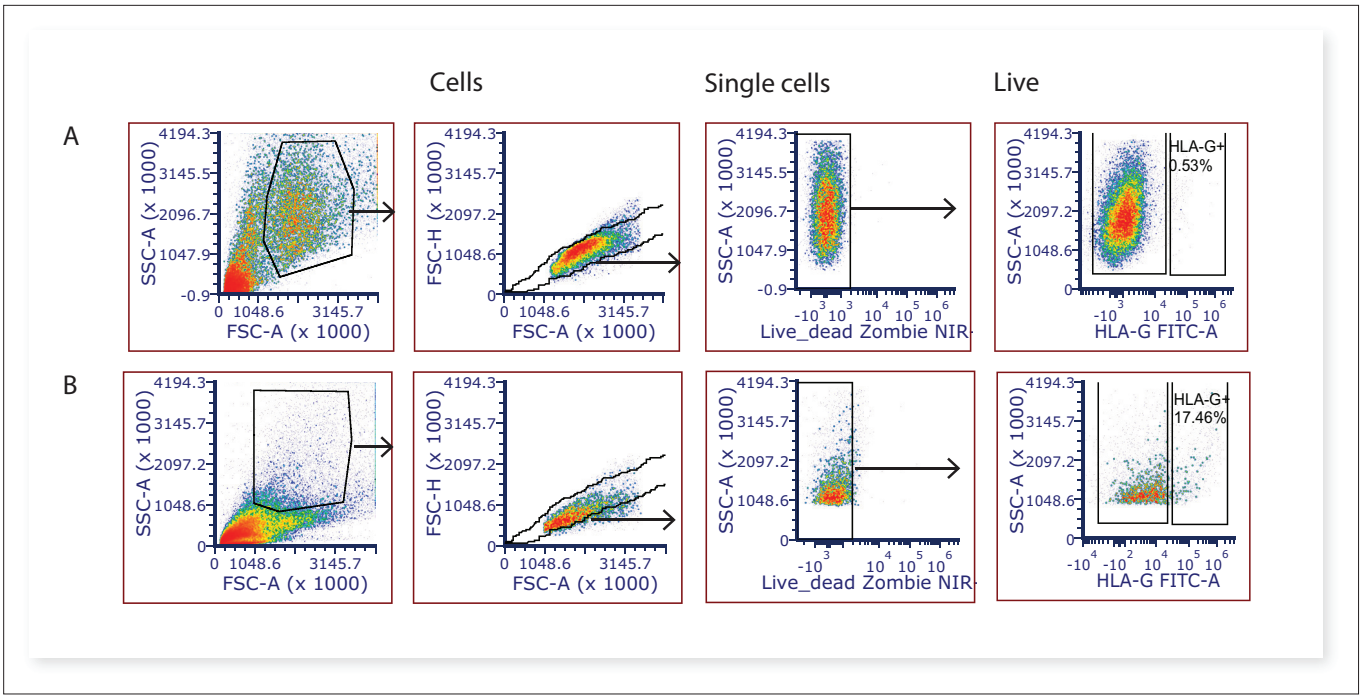

Figure 7. Representative 2-dimensional flow cytometry plots displaying the gating strategy used to assess the proportion of extravillous trophoblasts (HLAG +cells) in villous core digests. (**A**) Villous core cells and, (**B**) cells from the first digest washing steps known to contain extravillous trophoblasts were used as a positive control.

core cells with the extravillous trophoblast marker HLA-G (MEM-G/9)-FITC 5 µg/ml (SAB4700315, Sigma-Aldrich, NZ). A mean of 0.95% ± 0.91% of the total live cells were HLAG + extravillous trophoblasts (***Figure 7***), and are thus unlikely to impact on downstream stromal analyses. FCS files relating to quantifying extravillous trophoblasts (HLA-G + cells) contamination in villous digests can be found on FlowRepository ID FR-FCM-Z5FV.

Multicolour panel design and optimisation

Panel One was designed for analysis on a three laser Cytek Aurora and aimed to characterise mesenchymal lineages but with specific design considerations for first trimester placental villous core cells (***Table 3***). First, antigens specific for cytotrophoblasts (an epithelial cell that is present around the outside of placental villi, identified by β4 integrin) or haematopoietic cells (CD235a, CD45) were incorporated to allow their exclusion from analysis. Then endothelial, mesenchymal, myofibroblast, and progenitor antigens were selected based on reported literature in the placental and mesenchymal fields, or included in an exploratory role based on reported antigen expression in other tissues or stem cell models (***Table 1*** and ***Table 3***).

The online Cytek Full Spectrum Viewer was used to identify fluorophores with distinct signatures that could be included in each panel. The panel was designed to spectrally spread out antigens with high density expression in order to prevent spectral overlap or interference. Where possible the brightest fluorophores were combined with the weakest antigens or where antigen was of special interest (ie PE) (***Ferrer-Font et al., 2020***). Conversely, where the targets of the antigen were highly expressed dim fluorophores were selected (ie CD34 PerCP).

Each antibody was titrated on first trimester placental villous core cells (***Table 3—source data 1*** and ***Table 3—source data 2***). For some antibodies the optimal dose was difficult to detect due to the different autofluorescence and size of cells. Therefore, forward scatter was often employed to look at different sized cells, or CD45/β4 integrin were used to exclude hematopoietic and cytotrophoblast cells that interfered with detection of optimal antibody concentration in cell populations of interest (***Table 3—source data 3***). Where required the specificity of the antibody was confirmed using immunofluorescence (***Figure 1***). Biological controls included stromal vascular fraction and peripheral blood mononuclear cells, as have been previously characterised (***Boss et al., 2020***).

Table 3. Panel One designed to assess villous core cells on a 3 L Cytek Aurora.
Beads = Anti Ms Ig CompBead Plus Set (BD, 560497).

Antibody	Fluorophore	Clone	Flow cytometry Dose (µL)	Reference control	Supplier
CD55	BB515	IA10	0.6	Villous core cells	Beckman Coulter
β4 integrin	FITC	450-9D	0.6	Villous core cells	Thermofisher
CD34	PerCP	581	0.3	Villous core cells	BD
CD36	PerCpVio700	REA760	0.6	Villous core cells	Miltenyi Biotec
VEGFR2	PE	7D4-6	0.6	Villous core cells	Biolegend
CD271	PE-CF594	C40-1457	0.6	Stromal vascular fraction	Biolegend
CD142	BB700	HTF-1	1.25	Villous core cells	BD
CD26	PE/Cy5	BA5b	0.15	Villous core cells	BD
PDPN	PE/Cy7	NC-08	0.3	Villous core cells	BD
CD248	Alexa Fluor 647	B1/35	0.6	Stromal vascular fraction	BD
CD41	APC	HIP8	0.3	Beads	BD
CD90	Alexa700	5E10	0.6	Villous core cells	Biolegend
CD39	BUV737	TU66	1.25	Beads	BD
ICAM1	APC/Fire750	HA58	2.5	Stromal vascular fraction	Biolegend
CD144	BV421	55–7 H1	1.25	Villous core cells	BD
CD235a	Pacific Blue	H1264	0.3	Villous core cells	BD
CD31	BV480	WM59	0.3	Villous core cells	BD
CD45	Krome-Orange	B61840	0.3	Villous core cells	Beckman Coulter
CD146	BV605	PIH12	0.3	Villous core cells	BD
CD117	BV650	104D2	0.3	Beads	BD
HLADR	BV750	L243	0.3	Villous core cells	BD
CD73	BV785	AD2	0.3	Villous core cells	BD

The online version of this article includes the following source data for table 3:

Source data 1. All antibodies used in Panel One were titrated on placental villous core digest cells.

Source data 2. Titration of additional antibodies, not contained in Panel One, required for the FACS sorting with Panel Two.

Source data 3. Representative images depicting how forward scatter (FSC) (A) or addition of cell-specific antibodies improved detection of appropriate doses for specific placental populations.

Spectral flow cytometry

Freshly isolated cells were blocked with 5 µL of Human TruStain FcX (Biolegend, USA) and 5 µL of True-Stain Monocyte Blocker (Biolegend, USA) on ice for 30 minutes. An antibody master mix containing antibodies listed in ***Table 3*** was prepared in 5 µl of Brilliant Stain Buffer (Biosciences, US) in order to block BD Horizon Brilliant fluorescent polymer dyes from interacting with each other. The master mix was added to the cells in blocking solution to make a final volume of 50 µl and incubated on ice for 30 minutes in the dark. Stained cells were washed with 1 mL of ice cold FACS buffer (PBS, 2 mM EDTA (Thermofisher, US) and 1% FBS (Thermofisher, NZ)) and centrifuged at 220xg for five minutes at 4 °C. The supernatant was decanted and the wash was repeated. Cells were then resuspended in 100 µl of FACS buffer and kept at 4 °C. DAPI (1:5000, Akoya Biosciences) was spiked into FACS tubes directly prior to analysis on a Cytek Aurora in order to detect live/dead cells. Spectral data was processed using the Cytek SpectroFlo Software Package.

Fluorescence minus one (FMO) experiments were performed to accurately gate cell populations and to assess fluorophore spreading error where required. This was completed by creating a master

Table 4. Composition of Panel Two.
This panel was developed to sort CD73 + CD90 + and podoplanin + CD36 + cells from placental villous core using a BD FACS Aria II.

Antibody	Fluorophore	Clone	Dose (µL)	Supplier
CD45	FITC	HI30	0.3	BD
PDPN	PE	NC-08	0.3	Biolegend
CD26	PE/Cy7	BA5b	0.6	BD
CD271	PE/Dazzle 594	C40-1457	0.6	BD
CD144	PerCP-5.5	55–7 H1	0.6	BD
CD90	Alexa700	5E10	0.6	Biolegend
CD36	APC-Cy7	5–271	0.6	Biolegend
β4 integrin	APC	450-9D	0.6	Thermofisher
CD31	BV480	WM59	0.3	BD
CD73	BV785	AD2	0.3	BD
CD34	BUV395	581	1.25	BD

mix containing all the antibodies in the panel minus the antibody of interest. The FMO was then compared to the full panel stain to identify whether the expression detected by that antibody is only present in the full stain, and therefore represents true positive expression. FCS files relating to the characterisation of primary cells can be found on FlowRepository ID FR-FCM-Z4TJ.

Data analysis

Spectrally unmixed FCS files were exported from SpectroFlo and either manually analysed using 2 dimensional dot plots with FCS Express (v7) or uploaded onto Cytobank, a platform enabling datasets to be analysed by algorithms designed to assess high dimensional flow cytometry datasets https://cytobank.org/ (***Kotecha et al., 2010***). In Cytobank, debris, doublets, and dead cells were excluded by manual gating then equal sampling (200,000 villous cells from each placentae were selected, n=5). ViSNE enables visualisation of high dimensional data in two dimensions, each cell is displayed as a point on a scatter-like plot where cells with similar antigen expression will group closely and dissimilar cells will be further apart.

For further analysis of subsets of core populations, cytotrophoblasts (identified by their expression of β4 integrin) and hematopoietic cells (identified by their expression of CD45 or CD235a) were excluded by gating. Villus core subsets were then interrogated using expression heatmaps (Cytobank) and flow cytometry plots (FCS Express7). The gating strategy employed to identify populations is displayed in ***Figure 3***.

FACS sorting and in vitro culture of mesenchymal populations

In order to determine in vitro characteristics of Subset Two ($CD73^+CD90^+$) and Subset Four ($podoplanin^+CD36^+$) these populations were isolated using FACS for in vitro culture. To do this, placental villous core cells were isolated and stained with Panel Two master mix (***Table 4***) using the same methods as above. Cells were resuspended in 500 µL of Sort Buffer (10% FBS, 2 mM EDTA in PBS) and incubated on ice until immediately prior to sorting. Subset Two ($CD73^+CD90^+$) and Subset Four ($podoplanin^+CD36^+$) were sorted into 5 mL FACS tubes containing endothelial basal media (EGM-2 medium without supplements added, Lonza, USA) supplemented with 10% FBS at 4 °C degrees. To sort cells of interest, the gating strategy displayed in ***Figure 3*** was used to exclude debris, doublets, dead cells, trophoblasts, and endothelial cells, before gating the populations of interest. For each population 3000 cells/cm^2 were seeded onto 24-well plates in EGM-2. After 7 days, the in vitro phenotype of cells was determined using Panel Three (***Table 5***). In brief, TryPLE express was used to detach cells from flasks. Cells were blocked and then stained with a master mix for Panel Three (***Table 5***) as described above. Placental MSCs were isolated in EGM-2 using an explant method as described in

Table 5. Composition of Panel Three.
This panel was designed to assess the phenotype of placental populations after culture in vitro using a three laser Cytek Aurora.

Antibody	Fluorophore	Clone	Dose	Supplier
CD34	PerCP	581	0.3	BD
CD36	PerCpVio700	REA760	0.6	Miltenyi Biotec
VEGFR2	PE	7D4-6	0.6	Biolegend
CD271	PE/Dazzle 594	C40-1457	0.6	Biolegend
CD142	BB700	HTF-1	1.25	BD
CD26	PE/Cy5	BA5b	0.15	BD
PDPN	PE/Cy7	NC-08	0.3	BD
CD90	Alexa700	5E10	0.6	Biolegend
CD144	BV421	55–7 H1	1.25	BD
CD31	BV480	WM59	0.3	BD
CD45	Krome-Orange	B61840	0.3	Beckman Coulter
CD146	BV605	PIH12	0.3	BD
HLADR	BV750	L243	0.3	BD
CD73	BV785	AD2	0.3	BD

our previous work (***Boss et al., 2020***) were assessed in parallel by flow cytometry. FCS files relating to the cultured experiments can be found on FlowRepository ID FR-FCM-Z4TL.

Immunocytochemistry

In order to determine the capacity of Subset Two ($CD73^+CD90^+$) and Subset Four ($podoplanin^+CD36^+$) to upregulate contractile markers, in a similar way to pMSCs (***Boss et al., 2020***), cells were FACS sorted (as above) and seeded into 96 well plates at 2000 cells/cm^2 in EGM-2, with medium replaced every 2–3 days. At day 7 medium was switched to advanced-DMEM/F12 or kept as EGM-2 for a further 7 days. At day 14 of culture, cells were fixed with methanol for 10 min, washed in PBS, then incubated in 10% normal goat serum in PBS-tween for 1 h at room temperature. Cells were incubated with primary antibodies either 5 µg/ml of anti-Calponin (Abcam-ab216651), 1 µg/ml anti-α-smooth muscle actin (αSMA) (Thermofisher Scientific, 14-9760-82) or 1 µg/ml anti-smooth muscle heavy chain 11 (Abcam-ab53219) or the relevant control antibodies rabbit IgG (Abacus, JI111036144) or mouse IgG (Abacus, JI115036146), for 1 h at room temperature. Endogenous peroxidase activity was quenched by addition of 3% H_2O_2 in methanol for 5 minutes. A Histostain Plus Bulk Kit (Invitrogen) with AEC chromogen (Invitrogen) was used as per the manufacturer's instructions to visualise antibody binding. Nuclei were counterstained with Gills II Haematoxylin (Sigma-Aldrich).

Acknowledgements

The authors would like to thank all the donors of placental tissue, and staff of Epsom Day Unit, Greenlane Clinical Centre and Auckland Medical Aid Centre for their assistance in recruiting patients to the study. This work was supported by a Health Research Council of New Zealand Sir Charles Hercus Research Fellowship (J James, 16/043). A Boss was supported by a University of Auckland Doctoral Scholarship and a University of Auckland Faculty of Science PhD output award.

Additional information

Funding

Funder	Grant reference number	Author
Health Research Council of New Zealand	16/043	Joanna L James
University of Auckland	Doctoral Scholarship	Anna Leabourn Boss

The funders had no role in study design, data collection and interpretation, or the decision to submit the work for publication.

Author contributions

Anna Leabourn Boss, Conceptualization, Data curation, Formal analysis, Investigation, Visualization, Methodology, Writing - original draft; Tanvi Damani, Investigation; Tayla J Wickman, Data curation, Formal analysis; Larry W Chamley, Writing – review and editing; Joanna L James, Conceptualization, Resources, Supervision, Funding acquisition, Methodology, Project administration, Writing – review and editing; Anna ES Brooks, Conceptualization, Resources, Software, Supervision, Funding acquisition, Methodology, Writing – review and editing

Author ORCIDs

Anna Leabourn Boss http://orcid.org/0000-0002-1943-4162
Anna ES Brooks http://orcid.org/0000-0003-3551-6982

Ethics

Human subjects: Placentae were collected following informed consent with approval from the Northern X Health and Disability Ethics Committee (NTX/12/06/057/AM09).

Decision letter and Author response

Decision letter https://doi.org/10.7554/eLife.76622.sa1
Author response https://doi.org/10.7554/eLife.76622.sa2

Additional files

Supplementary files

- Transparent reporting form

Data availability

FCS data files have been provided for flow cytometry presented in Figures 2-3 following the link: http://flowrepository.org/public_experiment_representations/FR-FCM-Z4TJ Figure 4: http://flowrepository.org/public_experiment_representations/FR-FCM-Z4TL Figure 7: http://flowrepository.org/public_experiment_representations/FR-FCM-Z5FV.

References

Abe K, Shoji M, Chen J, Bierhaus A, Danave I, Micko C, Casper K, Dillehay DL, Nawroth PP, Rickles FR. 1999. Regulation of vascular endothelial growth factor production and angiogenesis by the cytoplasmic tail of tissue factor. *PNAS* **96**:8663–8668. DOI: https://doi.org/10.1073/pnas.96.15.8663, PMID: 10411932

Abumaree MH, Al Jumah MA, Kalionis B, Jawdat D, Al Khaldi A, Abomaray FM, Fatani AS, Chamley LW, Knawy BA. 2013. Human placental mesenchymal stem cells (pMSCs) play a role as immune suppressive cells by shifting macrophage differentiation from inflammatory M1 to anti-inflammatory M2 macrophages. *Stem Cell Reviews and Reports* **9**:620–641. DOI: https://doi.org/10.1007/s12015-013-9455-2

Amir ED, Davis KL, Tadmor MD, Simonds EF, Levine JH, Bendall SC, Shenfeld DK, Krishnaswamy S, Nolan GP, Pe'er D. 2013. viSNE enables visualization of high dimensional single-cell data and reveals phenotypic heterogeneity of leukemia. *Nature Biotechnology* **31**:545–552. DOI: https://doi.org/10.1038/nbt.2594, PMID: 23685480

Astarita JL, Acton SE, Turley SJ. 2012. Podoplanin: emerging functions in development, the immune system, and cancer. *Frontiers in Immunology* **3**:283. DOI: https://doi.org/10.3389/fimmu.2012.00283, PMID: 22988448

Barilani M, Banfi F, Sironi S, Ragni E, Guillaumin S, Polveraccio F, Rosso L, Moro M, Astori G, Pozzobon M, Lazzari L. 2018. Low-affinity nerve growth factor receptor (cd271) heterogeneous expression in adult and fetal

mesenchymal stromal cells. *Scientific Reports* **8**:9321. DOI: https://doi.org/10.1038/s41598-018-27587-8, PMID: 29915318

Blocki A, Wang Y, Koch M, Peh P, Beyer S, Law P, Hui J, Raghunath M. 2013. Not all MSCs can act as pericytes: functional in vitro assays to distinguish pericytes from other mesenchymal stem cells in angiogenesis. *Stem Cells and Development* **22**:2347–2355. DOI: https://doi.org/10.1089/scd.2012.0415, PMID: 23600480

Boss A.L, Brooks AES, Chamley LW, James JL. 2020. Influence of culture media on the derivation and phenotype of fetal-derived placental mesenchymal stem/stromal cells across gestation. *Placenta* **101**:66–74. DOI: https://doi.org/10.1016/j.placenta.2020.09.002, PMID: 32932101

Boss AL, Chamley LW, Brooks AES, James JL. 2021. Differences in human placental mesenchymal stromal cells may impair vascular function in FGR. *Reproduction* **162**:319–330. DOI: https://doi.org/10.1530/REP-21-0226, PMID: 34397395

Brooks AES, Iminitoff M, Williams E, Damani T, Jackson-Patel V, Fan V, James J, Dunbar PR, Feisst V, Sheppard HM. 2020. Ex vivo human adipose tissue derived mesenchymal stromal cells (asc) are a heterogeneous population that demonstrate rapid culture-induced changes. *Frontiers in Pharmacology* **10**:1. DOI: https://doi.org/10.3389/fphar.2019.01695, PMID: 32153389

Burton GJ, Jauniaux E. 2018. Pathophysiology of placental-derived fetal growth restriction. *American Journal of Obstetrics and Gynecology* **218**:S745–S761. DOI: https://doi.org/10.1016/j.ajog.2017.11.577, PMID: 29422210

Castrechini NM, Murthi P, Gude NM, Erwich J, Gronthos S, Zannettino A, Brennecke SP, Kalionis B. 2010. Mesenchymal stem cells in human placental chorionic villi reside in a vascular Niche. *Placenta* **31**:203–212. DOI: https://doi.org/10.1016/j.placenta.2009.12.006, PMID: 20060164

Chang LH, Huang HS, Wu PT, Jou IM, Pan MH, Chang WC, Wang DDH, Wang JM. 2012. Role of macrophage CCAAT/enhancer binding protein delta in the pathogenesis of rheumatoid arthritis in collagen-induced arthritic mice. *PLOS ONE* **7**:e45378. DOI: https://doi.org/10.1371/journal.pone.0045378, PMID: 23028973

Chen CP, Liu SH, Huang JP, Aplin JD, Wu YH, Chen PC, Hu CS, Ko CC, Lee MY, Chen CY. 2009. Engraftment potential of human placenta-derived mesenchymal stem cells after in utero transplantation in rats. *Human Reproduction***24**:154–165. DOI: https://doi.org/10.1093/humrep/den356, PMID: 18845668

Christopherson KW, Hangoc G, Mantel CR, Broxmeyer HE. 2004. Modulation of hematopoietic stem cell homing and engraftment by CD26. Science **305**:1000–1003. DOI: https://doi.org/10.1126/science.1097071, PMID: 15310902

Cimini M, Kishore R. 2021. Role of podoplanin-positive cells in cardiac fibrosis and angiogenesis after ischemia. *Frontiers in Physiology* **12**:667278. DOI: https://doi.org/10.3389/fphys.2021.667278, PMID: 33912076

Consentius C, Mirenska A, Jurisch A, Reinke S, Scharm M, Zenclussen AC, Hennig C, Volk HD. 2018. In situ detection of CD73+ CD90+ CD105+ lineage: Mesenchymal stromal cells in human placenta and bone marrow specimens by chipcytometry. *Cytometry. Part A* **93**:889–893. DOI: https://doi.org/10.1002/cyto.a.23509, PMID: 30211969

Crisan M, Chen CW, Corselli M, Andriolo G, Lazzari L, Péault B. 2009. Perivascular multipotent progenitor cells in human organs. *Annals of the New York Academy of Sciences* **1176**:118–123. DOI: https://doi.org/10.1111/j.1749-6632.2009.04967.x, PMID: 19796239

Cruz-Tapias P, Castiblanco J, Anaya JM. 2013. Major histocompatibility complex: Antigen processing and presentation. Autoimmunity.

da Silva Meirelles L, Malta TM, de Deus Wagatsuma VM, Palma PVB, Araújo AG, Ribeiro Malmegrim KC, Morato de Oliveira F, Panepucci RA, Silva WA Jr, Kashima Haddad S, Covas DT. 2015. Cultured human adipose tissue pericytes and mesenchymal stromal cells display a very similar gene expression profile. *Stem Cells and Development* **24**:2822–2840. DOI: https://doi.org/10.1089/scd.2015.0153, PMID: 26192741

Dellschaft NS, Hutchinson G, Shah S, Jones NW, Bradley C, Leach L, Platt C, Bowtell R, Gowland PA. 2020. The haemodynamics of the human placenta in utero. *PLOS Biology* **18**:e3000676. DOI: https://doi.org/10.1371/journal.pbio.3000676, PMID: 32463837

Demir R, Seval Y, Huppertz B. 2007. Vasculogenesis and angiogenesis in the early human placenta. *Acta Histochemica* **109**:257–265. DOI: https://doi.org/10.1016/j.acthis.2007.02.008, PMID: 17574656

Dominici M, Le Blanc K, Mueller I, Slaper-Cortenbach I, Marini F, Krause D, Deans R, Keating A, Prockop D, Horwitz E. 2006. Minimal criteria for defining multipotent mesenchymal stromal cells. *The International Society for Cellular Therapy Position Statement. Cytotherapy* **8**:315–317. DOI: https://doi.org/10.1080/14653240600855905, PMID: 16923606

Du W, Li X, Chi Y, Ma F, Li Z, Yang S, Song B, Cui J, Ma T, Li J, Tian J, Yang Z, Feng X, Chen F, Lu S, Liang L, Han ZB, Han ZC. 2016a. VCAM-1+ placenta chorionic villi-derived mesenchymal stem cells display potent pro-angiogenic activity. *Stem Cell Research & Therapy* **7**:49. DOI: https://doi.org/10.1186/s13287-016-0297-0, PMID: 27044487

Du WJ, Chi Y, Yang ZX, Li ZJ, Cui JJ, Song BQ, Li X, Yang SG, Han ZB, Han ZC. 2016b. Heterogeneity of proangiogenic features in mesenchymal stem cells derived from bone marrow, adipose tissue, umbilical cord, and placenta. *Stem Cell Research & Therapy* **7**:163. DOI: https://doi.org/10.1186/s13287-016-0418-9, PMID: 27832825

Dye JF, Jablenska R, Donnelly JL, Lawrence L, Leach L, Clark P, Firth JA. 2001. Phenotype of the endothelium in the human term placenta. *Placenta* **22**:32–43. DOI: https://doi.org/10.1053/plac.2000.0579, PMID: 11162350

Farley AE, Graham CH, Smith GN. 2004. Contractile properties of human placental anchoring villi. *American Journal of Physiology. Regulatory, Integrative and Comparative Physiology* **287**:R680–R685. DOI: https://doi.org/10.1152/ajpregu.00222.2004, PMID: 15142834

Ferrer-Font L, Pellefigues C, Mayer JU, Small SJ, Jaimes MC, Price KM. 2020. Panel design and optimization for high-dimensional immunophenotyping assays using spectral flow cytometry. *Current Protocols in Cytometry* **92**:e70. DOI: https://doi.org/10.1002/cpcy.70, PMID: 32150355

Gao H, Volat F, Sandhow L, Galitzky J, Nguyen T, Esteve D, Åström G, Mejhert N, Ledoux S, Thalamas C, Arner P, Guillemot JC, Qian H, Rydén M, Bouloumié A. 2017. CD36 is a marker of human adipocyte progenitors with pronounced adipogenic and triglyceride accumulation potential. *Stem Cells* **35**:1799–1814. DOI: https://doi.org/10.1002/stem.2635, PMID: 28470788

Garcia-Alegria E, Menegatti S, Fadlullah MZH, Menendez P, Lacaud G, Kouskoff V. 2018. Early human hemogenic endothelium generates primitive and definitive hematopoiesis in vitro. *Stem Cell Reports* **11**:1061–1074. DOI: https://doi.org/10.1016/j.stemcr.2018.09.013, PMID: 30449319

Giannotta M, Trani M, Dejana E. 2013. VE-cadherin and endothelial adherens junctions: active guardians of vascular integrity. *Developmental Cell* **26**:441–454. DOI: https://doi.org/10.1016/j.devcel.2013.08.020, PMID: 24044891

Gillmore T, Farrell A, Alahari S, Sallais J, Kurt M, Park C, Ausman J, Litvack M, Post M, Caniggia I. 2022. Dichotomy in hypoxia-induced mitochondrial fission in placental mesenchymal cells during development and preeclampsia: consequences for trophoblast mitochondrial homeostasis. *Cell Death & Disease* **13**:191. DOI: https://doi.org/10.1038/s41419-022-04641-y, PMID: 35220394

Hanschkow M, Boulet N, Kempf E, Bouloumié A, Kiess W, Stein R, Körner A, Landgraf K. 2022. Expression of the adipocyte progenitor markers msca1 and cd36 is associated with adipose tissue function in children. *The Journal of Clinical Endocrinology and Metabolism* **107**:e836–e851. DOI: https://doi.org/10.1210/clinem/dgab630, PMID: 34448000

Hato T, Tabata M, Oike Y. 2008. The role of angiopoietin-like proteins in angiogenesis and metabolism. *Trends in Cardiovascular Medicine* **18**:6–14. DOI: https://doi.org/10.1016/j.tcm.2007.10.003, PMID: 18206803

Heinzelmann K, Lehmann M, Gerckens M, Noskovičová N, Frankenberger M, Lindner M, Hatz R, Behr J, Hilgendorff A, Königshoff M, Eickelberg O. 2018. Cell-surface phenotyping identifies CD36 and CD97 as novel markers of fibroblast quiescence in lung fibrosis. *American Journal of Physiology. Lung Cellular and Molecular Physiology* **315**:L682–L696. DOI: https://doi.org/10.1152/ajplung.00439.2017, PMID: 29952218

Hermiston ML, Xu Z, Weiss A. 2003. CD45: A critical regulator of signaling thresholds in immune cells. *Annual Review of Immunology* **21**:107–137. DOI: https://doi.org/10.1146/annurev.immunol.21.120601.140946, PMID: 12414720

Hubbard AK, Rothlein R. 2000. Intercellular adhesion molecule-1 (ICAM-1) expression and cell signaling cascades. *Free Radical Biology & Medicine* **28**:1379–1386. DOI: https://doi.org/10.1016/s0891-5849(00)00223-9, PMID: 10924857

Ingman K, Cookson V, Jones CJP, Aplin JD. 2010. Characterisation of Hofbauer cells in first and second trimester placenta: incidence, phenotype, survival in vitro and motility. *Placenta* **31**:535–544. DOI: https://doi.org/10.1016/j.placenta.2010.03.003, PMID: 20347485

James JL, Hurley DG, Gamage T, Zhang T, Vather R, Pantham P, Murthi P, Chamley LW. 2015. Isolation and characterisation of a novel trophoblast side-population from first trimester placentae. *Reproduction* **150**:449–462. DOI: https://doi.org/10.1530/REP-14-0646, PMID: 26248480

Kawai T, Choi U, Liu PC, Whiting-Theobald NL, Linton GF, Malech HL. 2007. Diprotin A infusion into nonobese diabetic/severe combined immunodeficiency mice markedly enhances engraftment of human mobilized CD34+ peripheral blood cells. *Stem Cells and Development* **16**:361–370. DOI: https://doi.org/10.1089/scd.2007.9997, PMID: 17610366

Kohnen G, Kertschanska S, Demir R, Kaufmann P. 1996. Placental villous stroma as a model system for myofibroblast differentiation. *Histochemistry and Cell Biology* **105**:415–429. DOI: https://doi.org/10.1007/BF01457655, PMID: 8791101

Kotecha N, Krutzik PO, Irish JM. 2010. Web-based analysis and publication of flow cytometry experiments. *Current Protocols in Cytometry* **10**:s53. DOI: https://doi.org/10.1002/0471142956.cy1017s53, PMID: 20578106

Kozlowska U, Krawczenko A, Futoma K, Jurek T, Rorat M, Patrzalek D, Klimczak A. 2019. Similarities and differences between mesenchymal stem/progenitor cells derived from various human tissues. *World Journal of Stem Cells* **11**:347–374. DOI: https://doi.org/10.4252/wjsc.v11.i6.347, PMID: 31293717

Kumar A, D'Souza SS, Moskvin OV, Toh H, Wang B, Zhang J, Swanson S, Guo L-W, Thomson JA, Slukvin II. 2017. Specification and diversification of pericytes and smooth muscle cells from mesenchymoangioblasts. *Cell Reports* **19**:1902–1916. DOI: https://doi.org/10.1016/j.celrep.2017.05.019, PMID: 28564607

Kusuma GD, Abumaree MH, Pertile MD, Kalionis B. 2018. Isolation and characterization of mesenchymal stem/stromal cells derived from human third trimester placental chorionic villi and decidua basalis. *Methods in Molecular Biology***1710**:247–266. DOI: https://doi.org/10.1007/978-1-4939-7498-6_19, PMID: 29197008

Lax S, Hardie DL, Wilson A, Douglas MR, Anderson G, Huso D, Isacke CM, Buckley CD. 2010. The pericyte and stromal cell marker CD248 (endosialin) is required for efficient lymph node expansion. *European Journal of Immunology* **40**:1884–1889. DOI: https://doi.org/10.1002/eji.200939877, PMID: 20432232

Leroyer AS, Blin MG, Bachelier R, Bardin N, Blot-Chabaud M, Dignat-George F. 2019. CD146 (cluster of differentiation 146). *Arteriosclerosis, Thrombosis, and Vascular Biology* **39**:1026–1033. DOI: https://doi.org/10.1161/ATVBAHA.119.312653, PMID: 31070478

Li W, Ferkowicz MJ, Johnson SA, Shelley WC, Yoder MC. 2005. Endothelial cells in the early murine yolk sac give rise to CD41-expressing hematopoietic cells. *Stem Cells and Development* **14**:44–54. DOI: https://doi.org/10.1089/scd.2005.14.44, PMID: 15725743

Lin CS, Ning H, Lin G, Lue TF. 2012. Is CD34 truly a negative marker for mesenchymal stromal cells? *Cytotherapy* **14**:1159–1163. DOI: https://doi.org/10.3109/14653249.2012.729817, PMID: 23066784

Link A, Hardie DL, Favre S, Britschgi MR, Adams DH, Sixt M, Cyster JG, Buckley CD, Luther SA. 2011. Association of T-zone reticular networks and conduits with ectopic lymphoid tissues in mice and humans. *The American Journal of Pathology* **178**:1662–1675. DOI: https://doi.org/10.1016/j.ajpath.2010.12.039, PMID: 21435450

Lv FJ, Tuan RS, Cheung KMC, Leung VYL, Soleti A, Navone S. 2014. Concise review: the surface markers and identity of human mesenchymal stem cells. *Stem Cells* **32**:1408–1419. DOI: https://doi.org/10.1002/stem.1681, PMID: 24578244

Mao B, Huang S, Lu X, Sun W, Zhou Y, Pan X, Yu J, Lai M, Chen B, Zhou Q, Mao S, Bian G, Zhou J, Nakahata T, Ma F. 2016. Early development of definitive erythroblasts from human pluripotent stem cells defined by expression of glycophorin A/CD235a, CD34, and CD36. *Stem Cell Reports* **7**:869–883. DOI: https://doi.org/10.1016/j.stemcr.2016.09.002, PMID: 27720903

Marelli-Berg FM, Clement M, Mauro C, Caligiuri G. 2013. An immunologist's guide to CD31 function in T-cells. *Journal of Cell Science* **126**:2343–2352. DOI: https://doi.org/10.1242/jcs.124099, PMID: 23761922

Mezawa Y, Daigo Y, Takano A, Miyagi Y, Yokose T, Yamashita T, Morimoto C, Hino O, Orimo A. 2019. CD26 expression is attenuated by TGF-β and SDF-1 autocrine signaling on stromal myofibroblasts in human breast cancers. *Cancer Medicine* **8**:3936–3948. DOI: https://doi.org/10.1002/cam4.2249, PMID: 31140748

Mezheyeuski A, Segersten U, Leiss LW, Malmström P-U, Hatina J, Östman A, Strell C. 2020. Fibroblasts in urothelial bladder cancer define stroma phenotypes that are associated with clinical outcome. *Scientific Reports* **10**:1–12. DOI: https://doi.org/10.1038/s41598-019-55013-0, PMID: 31937798

Moll G, Drzeniek N, Kamhieh-Milz J, Geissler S, Volk HD, Reinke P. 2020. MSC therapies for covid-19: importance of patient coagulopathy, thromboprophylaxis, cell product quality and mode of delivery for treatment safety and efficacy. *Frontiers in Immunology* **11**:1091. DOI: https://doi.org/10.3389/fimmu.2020.01091, PMID: 32574263

Morrissey JH. 2004. Tissue factor: A key molecule in hemostatic and nonhemostatic systems. *International Journal of Hematology* **79**:103–108. DOI: https://doi.org/10.1532/ijh97.03167, PMID: 15005335

Nazari B, Rice LM, Stifano G, Barron AMS, Wang YM, Korndorf T, Lee J, Bhawan J, Lafyatis R, Browning JL. 2016. Altered dermal fibroblasts in systemic sclerosis display podoplanin and CD90. *The American Journal of Pathology* **186**:2650–2664. DOI: https://doi.org/10.1016/j.ajpath.2016.06.020, PMID: 27565038

Onak Kandemir N, Barut F, Barut A, Birol İE, Dogan Gun B, Ozdamar SO. 2019. Biological importance of podoplanin expression in chorionic villous stromal cells and its relationship to placental pathologies. *Scientific Reports* **9**:1–9. DOI: https://doi.org/10.1038/s41598-019-50652-9, PMID: 31578434

Ou X, O'Leary HA, Broxmeyer HE. 2013. Implications of DPP4 modification of proteins that regulate stem/progenitor and more mature cell types. *Blood* **122**:161–169. DOI: https://doi.org/10.1182/blood-2013-02-487470, PMID: 23637126

Papait A, Vertua E, Magatti M, Ceccariglia S, De Munari S, Silini AR, Sheleg M, Ofir R, Parolini O. 2020. Mesenchymal stromal cells from fetal and maternal placenta possess key similarities and differences: potential implications for their applications in regenerative medicine. *Cells* **9**:E127. DOI: https://doi.org/10.3390/cells9010127, PMID: 31935836

Pelekanos RA, Sardesai VS, Futrega K, Lott WB, Kuhn M, Doran MR. 2016. Isolation and expansion of mesenchymal stem/stromal cells derived from human placenta tissue. *Journal of Visualized Experiments* **1**:54204. DOI: https://doi.org/10.3791/54204, PMID: 27340821

Pinto MT, Covas DT, Kashima S, Rodrigues CO. 2016. Endothelial mesenchymal transition: comparative analysis of different induction methods. *Biological Procedures Online* **18**:10. DOI: https://doi.org/10.1186/s12575-016-0040-3, PMID: 27127420

Quintanilla M, Montero-Montero L, Renart J, Martín-Villar E. 2019. Podoplanin in inflammation and cancer. *International Journal of Molecular Sciences* **20**:707. DOI: https://doi.org/10.3390/ijms20030707, PMID: 30736372

Reimegård J, Tarbier M, Danielsson M, Schuster J, Baskaran S, Panagiotou S, Dahl N, Friedländer MR, Gallant CJ. 2021. A combined approach for single-cell mRNA and intracellular protein expression analysis. *Communications Biology* **4**:624. DOI: https://doi.org/10.1038/s42003-021-02142-w, PMID: 34035432

Roh M, Wainwright DA, Wu JD, Wan Y, Zhang B. 2020. Targeting CD73 to augment cancer immunotherapy. *Current Opinion in Pharmacology* **53**:66–76. DOI: https://doi.org/10.1016/j.coph.2020.07.001, PMID: 32777746

Rönnstrand L. 2004. Signal transduction via the stem cell factor receptor/c-Kit. *Cellular and Molecular Life Sciences* **61**:2535–2548. DOI: https://doi.org/10.1007/s00018-004-4189-6, PMID: 15526160

Ruiz-Argüelles A, Llorente L. 2007. The role of complement regulatory proteins (CD55 and CD59) in the pathogenesis of autoimmune hemocytopenias. *Autoimmunity Reviews* **6**:155–161. DOI: https://doi.org/10.1016/j.autrev.2006.09.008, PMID: 17289551

Saldanha-Araujo F, Ferreira FIS, Palma PV, Araujo AG, Queiroz RHC, Covas DT, Zago MA, Panepucci RA. 2011. Mesenchymal stromal cells up-regulate CD39 and increase adenosine production to suppress activated T-lymphocytes. *Stem Cell Research* **7**:66–74. DOI: https://doi.org/10.1016/j.scr.2011.04.001, PMID: 21546330

Sidney LE, Branch MJ, Dunphy SE, Dua HS, Hopkinson A. 2014. Concise review: evidence for CD34 as a common marker for diverse progenitors. *Stem Cells* **32**:1380–1389. DOI: https://doi.org/10.1002/stem.1661, PMID: 24497003

Silverstein RL, Febbraio M. 2009. CD36, a scavenger receptor involved in immunity, metabolism, angiogenesis, and behavior. *Science Signaling* **2**:re3. DOI: https://doi.org/10.1126/scisignal.272re3, PMID: 19471024

Soare A, Györfi HA, Matei AE, Dees C, Rauber S, Wohlfahrt T, Chen C-W, Ludolph I, Horch RE, Bäuerle T, von Hörsten S, Mihai C, Distler O, Ramming A, Schett G, Distler JHW. 2020. Dipeptidylpeptidase 4 as a marker of activated fibroblasts and a potential target for the treatment of fibrosis in systemic sclerosis. *Arthritis & Rheumatology* **72**:137–149. DOI: https://doi.org/10.1002/art.41058, PMID: 31350829

Soland MA, Bego M, Colletti E, Zanjani ED, St Jeor S, Porada CD, Almeida-Porada G. 2013. Mesenchymal stem cells engineered to inhibit complement-mediated damage. *PLOS ONE* **8**:e60461. DOI: https://doi.org/10.1371/journal.pone.0060461, PMID: 23555976

Suchanski J, Tejchman A, Zacharski M, Piotrowska A, Grzegrzolka J, Chodaczek G, Nowinska K, Rys J, Dziegiel P, Kieda C, Ugorski M. 2017. Podoplanin increases the migration of human fibroblasts and affects the endothelial cell network formation: A possible role for cancer-associated fibroblasts in breast cancer progression. *PLOS ONE* **12**:e0184970. DOI: https://doi.org/10.1371/journal.pone.0184970, PMID: 28938000

Suryawanshi H, Morozov P, Straus A, Sahasrabudhe N, Max KEA, Garzia A, Kustagi M, Tuschl T, Williams Z. 2018. A single-cell survey of the human first-trimester placenta and decidua. *Science Advances* **4**:eaau4788. DOI: https://doi.org/10.1126/sciadv.aau4788, PMID: 30402542

Takeda A, Hollmén M, Dermadi D, Pan J, Brulois KF, Kaukonen R, Lönnberg T, Boström P, Koskivuo I, Irjala H, Miyasaka M, Salmi M, Butcher EC, Jalkanen S. 2019. Single-Cell survey of human lymphatics unveils marked endothelial cell heterogeneity and mechanisms of homing for neutrophils. *Immunity* **51**:561–572. DOI: https://doi.org/10.1016/j.immuni.2019.06.027, PMID: 31402260

Tomkowicz B, Rybinski K, Sebeck D, Sass P, Nicolaides NC, Grasso L, Zhou Y. 2010. Endosialin/TEM-1/CD248 regulates pericyte proliferation through PDGF receptor signaling. *Cancer Biology & Therapy* **9**:908–915. DOI: https://doi.org/10.4161/cbt.9.11.11731, PMID: 20484976

Van Handel BJ, Prashad S, Huang A, Hamalainen E, Chen A, Mikkola HKA. 2007. The first trimester human placenta is a site of primitive red blood cell maturation First Trimester Human Placenta Is a Site of Primitive Red Blood Cell Maturation. *Blood* **110**:2224. DOI: https://doi.org/10.1182/blood.V110.11.2224.2224

Vijay J, Gauthier MF, Biswell RL, Louiselle DA, Johnston JJ, Cheung WA, Belden B, Pramatarova A, Biertho L, Gibson M, Simon MM, Djambazian H, Staffa A, Bourque G, Laitinen A, Nystedt J, Vohl MC, Fraser JD, Pastinen T, Tchernof A, et al. 2019. Single-cell analysis of human adipose tissue identifies depot and disease specific cell types. *Nature Metabolism* **2**:97–109. DOI: https://doi.org/10.1038/s42255-019-0152-6, PMID: 32066997

Viswanathan S, Shi Y, Galipeau J, Krampera M, Leblanc K, Martin I, Nolta J, Phinney DG, Sensebe L. 2019. Mesenchymal stem versus stromal cells: international society for cell & gene therapy (isct) mesenchymal stromal cell committee position statement on nomenclature. *Cytotherapy* **21**:1019–1024. DOI: https://doi.org/10.1016/j.jcyt.2019.08.002, PMID: 31526643

Wang Y, Sun J, Gu Y, Zhao S, Groome LJ, Alexander JS. 2011. D2-40/podoplanin expression in the human placenta. *Placenta* **32**:27–32. DOI: https://doi.org/10.1016/j.placenta.2010.10.014, PMID: 21095001

Ward LSC, Sheriff L, Marshall JL, Manning JE, Brill A, Nash GB, McGettrick HM. 2019. Podoplanin regulates the migration of mesenchymal stromal cells and their interaction with platelets. *Journal of Cell Science* **132**:jcs222067. DOI: https://doi.org/10.1242/jcs.222067, PMID: 30745334

Worthen CA, Cui Y, Orringer JS, Johnson TM, Voorhees JJ, Fisher GJ. 2020. CD26 identifies a subpopulation of fibroblasts that produce the majority of collagen during wound healing in human skin. *The Journal of Investigative Dermatology* **140**:2515–2524.. DOI: https://doi.org/10.1016/j.jid.2020.04.010, PMID: 32407715

Yoder MC. 2009. Defining human endothelial progenitor cells. *Journal of Thrombosis and Haemostasis* **7 Suppl 1**:49–52. DOI: https://doi.org/10.1111/j.1538-7836.2009.03407.x, PMID: 19630767

Zhang EG, Burton GJ, Smith SK, Charnock-Jones DS. 2002. Placental vessel adaptation during gestation and to high altitude: changes in diameter and perivascular cell coverage. *Placenta* **23**:751–762. DOI: https://doi.org/10.1016/s0143-4004(02)90856-8, PMID: 12398815

Zhao H, Bo C, Kang Y, Li H. 2017. What else can CD39 tell us? *Frontiers in Immunology* **8**:727. DOI: https://doi.org/10.3389/fimmu.2017.00727, PMID: 28690614